Estuaries and Coasts (2016) 39:1050–1071
DOI 10.1007/s12237-016-0071-7

Variable Nitrification Rates Across Environmental Gradients in Turbid, Nutrient-Rich Estuary Waters of San Francisco Bay

Julian Damashek[1] · **Karen L. Casciotti**[1] · **Christopher A. Francis**[1]

Received: 13 April 2015 / Revised: 18 January 2016 / Accepted: 26 January 2016 / Published online: 18 February 2016

Abstract Understanding rates of nitrogen cycling in estuaries is crucial for understanding their productivity and resilience to eutrophication. Nitrification, the microbial oxidation of ammonia to nitrite and nitrate, links reduced and oxidized forms of inorganic nitrogen and is therefore an important step of the nitrogen cycle. However, rates of nitrification in estuary waters are poorly characterized. In fall and winter of 2011–2012, we measured nitrification rates throughout the water column of all major regions of San Francisco Bay, a large, turbid, nutrient-rich estuary on the west coast of North America. Nitrification rates were highest in regions furthest from the ocean, including many samples with rates higher than those typically measured in the sea. In bottom waters, nitrification rates were commonly at least twice the magnitude of surface rates. Strong positive correlations were found between nitrification and both suspended particulate matter and ammonium concentration. Our results are consistent with previous studies documenting high nitrification rates in brackish, turbid regions of other estuaries, many of which also showed correlations with suspended sediment and ammonium concentrations. Overall, nitrification in estuary waters appears to play a significant role in the estuarine nitrogen cycle, though the maximum rate of nitrification can differ dramatically between estuaries.

Keywords Nitrification · Biogeochemistry · Ammonia oxidation · Ammonium · Nitrogen · Estuary

Communicated by Carolyn A. Currin

Electronic supplementary material The online version of this article (doi:10.1007/s12237-016-0071-7) contains supplementary material, which is available to authorized users.

✉ Christopher A. Francis
caf@stanford.edu

Julian Damashek
juliand@stanford.edu

Karen L. Casciotti
kcasciotti@stanford.edu

[1] Department of Earth System Science, Stanford University, 473 Via Ortega, Room 140, Stanford, CA 94305-4216, USA

Introduction

Since the development of industrial methods to fix dinitrogen (N_2) gas, the global nitrogen (N) cycle has been heavily perturbed (Rockström et al. 2009). Estuaries, in particular, can be highly impacted by coastal nutrient pollution and eutrophication, due to their locations near dense population centers and at the mouths of large watersheds (Bricker et al. 2008). Estuaries are very diverse ecosystems, with widely varying levels of nutrients, productivity, turbidity, and tidal range. Because of this, relationships between N supply and productivity in estuaries are not straightforward, complicating efforts to manage eutrophication via nutrient reductions (Paerl 2009). High N inputs can have cascading effects on phytoplankton growth and ecosystem metabolism; thus, understanding the productivity and food web structure of any estuary requires a comprehension of N cycling rates, especially in ecosystems heavily impacted by nutrient pollution. Additionally, links between estuary N cycles and regional changes such as increasing temperatures, sea-level rise, and changing species phenology remain largely unexplored (Rabalais et al. 2009; Najjar et al. 2010). Despite the mantra of estuaries acting as ecological "filters" between the land and the sea (Schubel and Kennedy 1984), rates of N cycling processes in many estuaries are not well constrained. Studies of biogeochemical processes in a variety of estuaries are needed

to determine whether general patterns exist and to set baselines from which future changes can be compared.

Nitrogen in aquatic ecosystems exists in numerous forms, including inorganic ions across a range of oxidation states and organic molecules such as amino acids, urea, and polyamines. With the exception of photosynthetic uptake, most inorganic N cycling pathways occur due to dissimilatory microbial metabolic reactions (Ward 2012). Nitrification is the microbially catalyzed oxidation of ammonia (NH_3) to nitrite (NO_2^-), followed by oxidation of NO_2^- to nitrate (NO_3^-). These processes are carried out by distinct functional groups (or guilds) of organisms: ammonia-oxidizing bacteria (AOB) and archaea (AOA) convert ammonia to nitrite, while nitrite-oxidizing bacteria (NOB) oxidize nitrite to nitrate. As the primary link between reduced ammonium (NH_4^+) or NH_3 and the oxidized substrates (NO_3^- and NO_2^-) required for denitrification and anammox (the two microbial processes capable of converting inorganic N to N_2), nitrification is a critical component of the N cycle of any ecosystem.

Although estuaries typically sustain far greater N loads than marine waters, relatively few recent studies have measured nitrification rates in estuary waters. Measurements of pelagic estuarine nitrification have evolved from measuring carbon fixation (^{14}C uptake) or changes in bulk nutrient concentrations in combination with nitrification inhibitors (e.g., Somville 1984; Feliatra and Bianchi 1993) to ^{15}N-NH_4^+ tracer techniques, which tend to be more sensitive and require fewer assumptions about inhibitor efficiency in natural nitrifying populations (Hall 1984; Santoro et al. 2010) or ratios between carbon fixation and ammonia oxidation (Enoksson 1986; Andersson et al. 2006). For these reasons, tracer incubations have become the most common way to estimate instantaneous nitrification rates throughout the sea (e.g., Beman et al. 2008; Santoro et al. 2010; Newell et al. 2011; Füssel et al. 2012; Smith et al. 2015). Detection of nitrification using ^{15}N-NH_4^+ relies on measurement of ^{15}N in NO_2^- and NO_3^- (NO_X). Measurements of ^{15}N-NO_X include adaptations of the ammonia diffusion method (e.g., Brion et al. 2008), multi-step chemical extraction procedures involving capture of nitrite in an aniline dye and solvent extraction to measure ^{15}N-NO_X (e.g., Ward and Kilpatrick 1990), and the denitrifier method, which converts NO_X to nitrous oxide (N_2O) for isotopic analysis (Sigman et al. 2001). The denitrifier method provides some advantages in sample throughput and sensitivity of $^{15}N/^{14}N$ measurements, particularly at low rates of nitrification, allowing for detection of rates when changes in NO_X concentrations are below the detection limit of standard assays, as changes in $\delta^{15}N_{NOx}$ can be measured even when NO_X concentrations remain effectively constant and only trace amounts of ^{15}N-NH_4^+ were added (Santoro et al. 2013).

San Francisco Bay is the largest estuary on the west coast of North America and consists of two connected but distinct regions: South Bay is a relatively shallow polyhaline basin with little freshwater input and long residence times, while the northern regions (from Central Bay to the Sacramento River; Fig. 1) are a typical estuary gradient from high-salinity water in Central Bay to the Sacramento and San Joaquin Rivers, with the location of brackish zones in North Bay depending on river flow (Conomos et al. 1985). The main source of freshwater to the estuary is the Sacramento River, with additional small inputs from the San Joaquin River and regional creeks and streams. Tidal exchange occurs through the Golden Gate, a narrow strait joining Central Bay to the Pacific Ocean. North Bay is mostly shallow, and tidal forcing is strong, leading to a generally well-mixed water column (Kimmerer 2004). This estuary has been profoundly affected by human activities in a myriad of ways, including freshwater diversions, changes in sediment supply, rampant biological invasions, and augmented nutrient inputs from wastewater effluent and agricultural/urban runoff (Kimmerer 2004; Cloern and Jassby 2012). However, primary productivity in San Francisco Bay is generally low, in spite of plentiful nutrients, with phytoplankton biomass largely limited by light and top-down predation (Cole and Cloern 1984; Alpine and Cloern 1992). Therefore, while seminal studies of pelagic N cycling processes in other North American estuaries were undertaken decades ago (e.g., McCarthy et al. 1984; Berounsky and Nixon 1985; Lipschultz et al. 1986), relatively little is known about nutrient biogeochemistry in San Francisco Bay. Meanwhile, recent research has suggested an increasing vulnerability of San Francisco Bay to high nutrient loads: annual averages of chlorophyll in South Bay are increasing (Cloern et al. 2010), blooms of toxic cyanobacteria are common in freshwater regions (Lehman et al. 2005), and altered nutrient stoichiometry may have cascading effects on the food web of the upper estuary (Glibert 2010). Renewed concern about eutrophication has refocused attention on N cycling in San Francisco Bay (e.g., Novick et al. 2014), yet nitrification in the water column remains an important unknown. Here, we used ^{15}N-NH_4^+ tracer incubations to measure nitrification rates in surface and bottom waters from all major regions of San Francisco Bay in the fall and winter of 2011–2012. These data represent a critical first step toward assessing the effects of this key process on the standing stocks and transformations of N throughout San Francisco Bay and in estuaries in general.

Materials and Methods

Sample Collection and Environmental Data

Water samples were collected from all major regions of San Francisco Bay on four cruises. Initial sampling on October 13, 2011, took place on the R/V *Questuary* (Romberg Tiburon Center, San Francisco State University), while the latter three cruises (October 18, 2011; December 13, 2011;

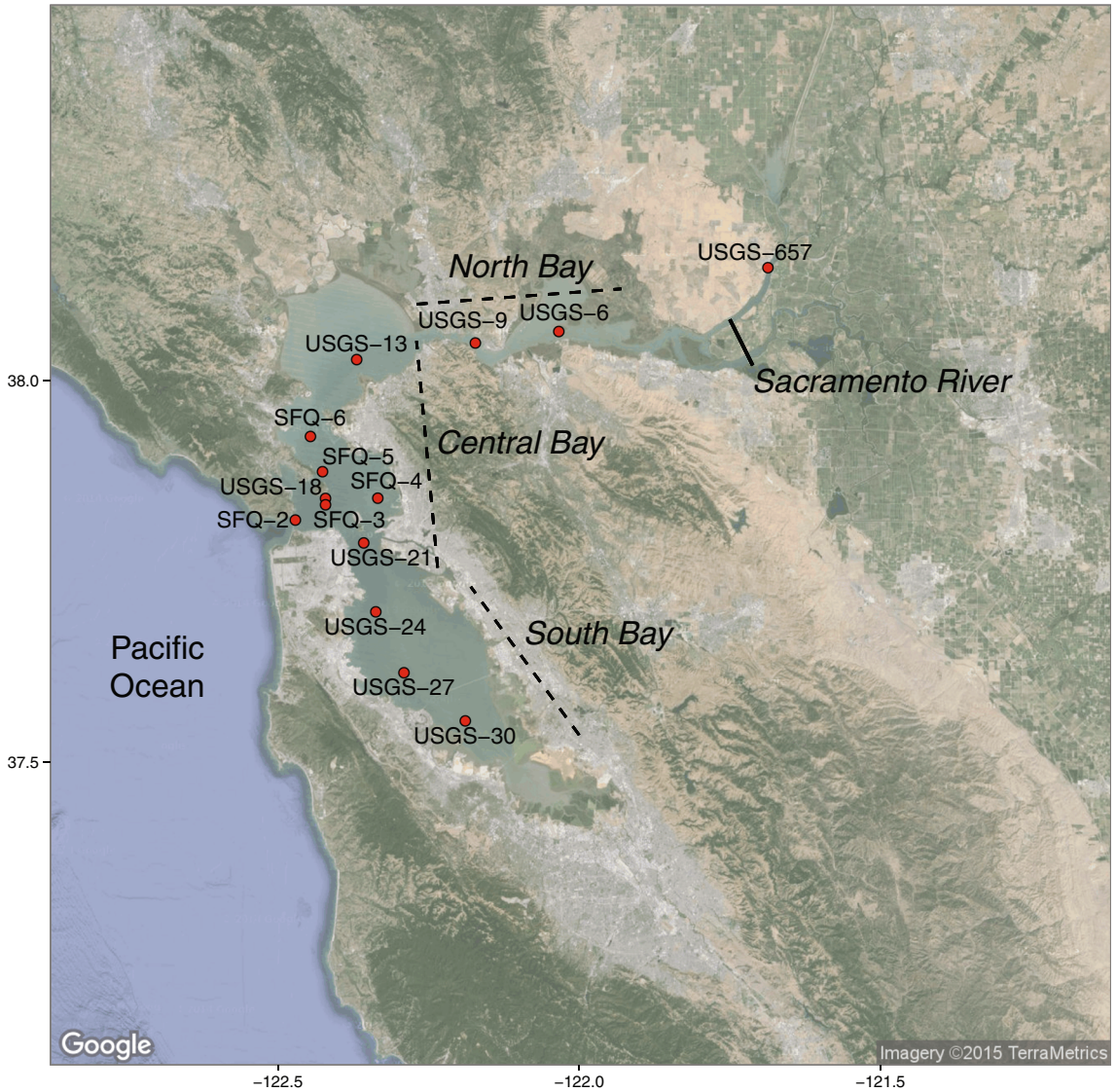

Fig. 1 Map of stations sampled throughout San Francisco Bay in fall and winter of 2011–2012. USGS stations were sampled on the *Polaris*, and SFQ stations were sampled on the *Questuary*

February 7, 2012) were aboard the R/V *Polaris* (USGS, Menlo Park). Fourteen stations were sampled in total (Fig. 1). Onboard the *Questuary*, water samples were collected from 1 to 3 depths using a Seabird Electronics SB-32 rosette mounted with six 3-L Niskin bottles. Vertical profiles of temperature and salinity, turbidity, photosynthetically active radiation (PAR), and chlorophyll were obtained from a Seabird SBE-19*plus* CTD, D&A OBS-3 turbidity sensor, Li-Cor LI-193 PAR sensor, and a WETStar fluorometer, respectively, mounted on the rosette. Light attenuation coefficients (k_d) were calculated as the slope of a regression line of natural log-transformed PAR versus depth. Onboard the *Polaris*, surface water samples (2 m depth) were collected from a continuous bow pump, and bottom-water samples (1 m above the sediment bed) were collected using a handheld Niskin bottle. Environmental parameters (excluding nutrient data) were collected by using a modified Seabird CTD and were downloaded from the USGS Water Quality of San Francisco Bay database (http://sfbay.wr.usgs.gov/access/wqdata; for detail on *Polaris* field methods, see http://sfbay.wr.usgs.gov/access/wqdata/overview/measure/index.html). All salinity data were measured using the Practical Salinity Scale. Delta outflow data were downloaded from the California Department of Water Resources Dayflow database (http://www.water.ca.gov/dayflow/). Nutrient samples were filtered (0.2-μm pore size) and immediately frozen on dry ice prior to storage at −20 °C. Nitrate and nitrite were measured using a Unity Scientific SmartChem 200 Discrete Analyzer, following standard procedures. Ammonium was measured using the salicylate-hypochlorite method (Bower and Holm-Hansen 1980).

Due to a lack of direct suspended particulate matter (SPM) measurements taken from *Questuary* stations, nitrification

rates measured on the *Questuary* could not be directly compared with SPM concentrations as done on the *Polaris* cruises using SPM data downloadad from the USGS database. To enable comparison, we created a simple model to estimate SPM concentrations from *Questuary* stations based on k_d and chlorophyll concentrations, which were measured on both ships. Since the only cruise on the *Questuary* took place in October 2011, we downloaded surface data collected on the *Polaris* from October 6 to November 4, 2011. Samples from Lower South Bay were excluded, due to anomalously high SPM concentrations and a paucity of k_d data from this region. Multiple linear regression models were constructed to explain the variability in k_d using SPM and chlorophyll concentrations (as measured directly on the *Polaris*), which were selected due to their potential ability to increase turbidity and thus affect k_d (Cloern 1987; Devlin et al. 2009). The final model was solved to calculate surface SPM concentrations, validated by comparing modeled and measured (i.e., database) SPM concentrations for *Polaris* cruises from September 20 and November 15, 2011, and used to calculate surface SPM concentrations at *Questuary* stations. Modeled surface SPM concentrations were scaled through the water column by assuming a 1:1 correlation between measured turbidity and calculated SPM.

Nitrification Rates

Nitrification was measured via ^{15}N-NH_4^+ tracer incubations similar to previously published methods (Santoro et al. 2010; Smith et al. 2014b). Water samples were amended with ^{15}N-NH_4Cl (99 atom% ^{15}N) at approximately 10 % of the ambient NH_4^+ concentration, gently mixed, and partitioned into duplicate 250-mL opaque HDPE bottles, which were held at ambient surface temperatures for 24 h in a flow-through polycarbonate deck incubator. Immediately following tracer addition and after 24 h, incubations were subsampled for $^{15}N/^{14}N$ isotope measurements of the NO_X pool ($\delta^{15}N_{NOx}$) by syringe filtration (0.2-μm pore size). Filtered samples were frozen on dry ice prior to storage at −20 °C. In addition to endpoint sampling, numerous incubations were sampled one to two additional times during the 24-h incubation period to assess the linearity of changes in $\delta^{15}N_{NOx}$ over time.

The bacterial denitrifier method was used to measure $\delta^{15}N_{NOx}$ (Sigman et al. 2001). Following bacterial conversion of NO_X to N_2O, isotopic ratios were measured using a Finnigan Delta^{PLUS} isotope ratio mass spectrometer (McIlvin and Casciotti 2011). Nitrate isotope references USGS-32, USGS-34, and USGS-35 were analyzed every nine samples to calibrate measured values. Given a measured $\delta^{15}N$ (‰) value, the atom ratio ^{15}N (AR_{15N}) was defined as follows:

$$AR_{15N} = \frac{^{15}N}{^{14}N} = \frac{(\delta^{15}N)(AR_{std})}{1000} + AR_{std} \quad (1)$$

assuming a reference (N_2 gas) atom ratio AR_{std} of 0.0036765 (Junk and Svec 1958). Calculated atom ratios of NO_X ($AR_{15N\text{-}NOx}$) were converted to atom fraction ^{15}N ($AF_{15N\text{-}NOx}$) using the following equation:

$$AF_{15N-NOx} = \frac{^{15}N_{NOx}}{^{14}N_{NOx} + ^{15}N_{NOx}} = \frac{AR_{15N-NOx}}{1 + AR_{15N-NOx}} \quad (2)$$

Nitrification rates (R_{nit}) were calculated using an endpoint model to estimate the flux of N from the NH_4^+ pool to the NO_X pool over time. This calculation (Eq. 3) was modified from models calculating phytoplankton nutrient uptake rates and is analogous to the "biomass-specific uptake rate" reported in the phytoplankton literature (e.g., Ward et al. 1989; Legendre and Gosselin 1996):

$$R_{nit} = \frac{([NO_X]) \times \left(AF_{15N-NO_{X_f}} - AF_{15N-NO_{X_i}}\right)}{\left(AF_{15N-NH_{4_{sp}}^+}\right) \times t}, \quad (3)$$

where $AF_{15N\text{-}NOxf}$ is the atom fraction $^{15}NO_X$ at the final timepoint, $AF_{15N\text{-}NOxi}$ is the initial (unlabeled) atom fraction $^{15}NO_X$, $[NO_X]$ is the concentration of the NO_X pool, and $AF_{15N\text{-}NH4sp}$ is the atom fraction $^{15}NH_4^+$ following addition of the ^{15}N-NH_4Cl spike. $AF_{15N\text{-}NH4sp}$ was calculated using the following equation:

$$AF_{15N-NH_{4_{sp}}^+} = \frac{\left(\left[NH_{4_i}^+\right]\right)\left(AF_{15N-NH_{4_i}^+}\right) + \left(\left[NH_{4_{add}}^+\right]\right)\left(AF_{15N-NH_{4_{add}}^+}\right)}{\left[NH_{4_i}^+\right] + \left[NH_{4_{add}}^+\right]}, \quad (4)$$

assuming a background atom fraction $^{15}NH_4^+$ ($AF_{15N\text{-}NH4i}$) equal to the standard value of 0.003663 and an atom fraction $^{15}NH_4^+$ of the added spike ($AF_{15N\text{-}NH4add}$) equal to 0.99. $[NH_4^+{}_i]$ and $[NH_4^+{}_{add}]$ were the measured in situ (unspiked) ammonium concentration and the added spike concentration, respectively. Since changes in NO_X and ammonium concentrations in the incubations were below the detection limit of our techniques, we assumed constant concentrations throughout the incubation period. We also assumed that ammonium was not significantly fractionated by uptake or diluted by remineralization during incubations. The validity of an endpoint calculation was assessed by checking the linearity of $\delta^{15}N_{NOx}$ increases in numerous incubations. For samples with duplicate nitrification measurements, the reported value is the midpoint, and error bars represent the range.

Statistical Analyses

Statistical tests were calculated using R (R Core Team 2014). Comparisons of data between seasons used two-tailed Welch *t* tests via the *t.test*() function, with October samples grouped as "fall" and December and February grouped as "winter."

Comparisons between regions (South Bay, Central Bay, North Bay, and the Sacramento River) used one-way ANOVA F tests. Pairwise correlations were assessed with Spearman's rank correlation coefficient (Spearman's ρ). Principal component analysis (PCA) was conducted using the *rda*() function in the vegan package (Oksanen et al. 2013), using a table of z-transformed environmental data by sample as input. The z-transformation subtracts the mean value from each measurement and divides by the standard deviation, standardizing data across different scales (Legendre and Legendre 2012). PCA results are shown in scaling 1, where distances between points represent the Euclidean distance between samples in multidimensional space (Borcard et al. 2011). Figures were made using the ggplot2 and ggmap packages in R (Wickham 2009; Kahle and Wickham 2013).

Multiple linear regression modeling was conducted in R. Outliers in explanatory variables were visually identified using Cleveland dotplots generated using the *dotchart*() command, and variables were transformed, if necessary. Collinearity was assessed using a combination of pairplots and variance inflation factors (VIFs), using the functions *pairs*() and *corvif*(), respectively (Zuur et al. 2009). Variables were sequentially removed if VIFs indicated significant collinearity, with remaining VIFs then recalculated until VIFs were all <3 and pairplots suggested no significant correlations. Initial analyses were conducted using all non-collinear explanatory variables, and models were parsed using a stepwise forward-backward selection of nested models using the *step*() command. Final model selection was based on a decreased Akaike's An Information Criterion (AIC) values and increased adjusted r^2 values. Regression assumptions were checked visually using a scatterplot of residuals against fitted model values, a histogram of residuals, a quantile-quantile plot, and scatterplots of model residuals against each explanatory variable. Response or explanatory variables were transformed to eliminate patterns in residual plots, if necessary.

Results

Environmental Data

Salinity varied regionally ($F_{4,28}=112.2$, $p<0.001$) in San Francisco Bay, reflecting proximity to the dominant saltwater and freshwater sources (the Pacific Ocean and the Sacramento River, respectively; Fig. 2a, h). Highest salinity waters were in Central Bay, with a mean value of 28.2 (SD = 2.10, $n=20$), while mean salinity decreased only slightly in South Bay (mean ± SD = 27.6 ± 0.43, $n=4$; see Supp. Table 1 for environmental data from each sample). In contrast, salinity was notably lower and more variable in North Bay (13.2 ± 7.90, $n=4$) and nearly zero in the Sacramento River (0.1 ± 0.02, $n=5$), reflecting classical estuarine mixing of marine and fresh waters along the northern estuary (Fig. 2a). Water temperature did not vary regionally ($F_{4,28}=2.0$, $p=0.19$) but showed distinct differences between seasons ($t_{28.6}=20.0$, $p<0.001$): mean fall temperature was 17.3 ± 0.9 °C ($n=19$), while winter temperature was 10.9 ± 0.9 °C ($n=14$; Fig. 2b, i). Chlorophyll also varied by season, with slightly higher values in the fall (5.9 ± 4.0 mg m^{-3}, $n=19$) compared to winter (2.7 ± 0.8 mg m^{-3}, $n=14$; $t_{19.8}=3.4$, $p=0.003$; Fig. 2c, j). Several fall samples from Central Bay waters had chlorophyll concentrations ≥10 mg m^{-3}, with a maximum of 12.8 mg m^{-3} at Station SFQ-3 (Supp. Table 1).

All nutrients showed similar regional patterns through space and time (Fig. 2e–g), with high concentrations in South Bay and the Sacramento River (except for nitrite, which was elevated in South Bay but not the Sacramento River; Fig. 2f). Additionally, all nutrients had lower concentrations in fall compared to winter (Fig. 2l–n), showing the inverse pattern of temperature and chlorophyll. Ammonium showed strong regional variation ($F_{4,28}=8.4$, $p<0.001$), with high concentrations in the Sacramento River (14.2 ± 4.97 μM, $n=5$) and South Bay (12.3 ± 4.73 μM, $n=4$) and lower values in North Bay (9.4 ± 2.51 μM, $n=4$) and Central Bay (6.1 ± 2.59 μM, $n=20$; Fig. 2e, Supp. Table 1). Nitrate also varied regionally ($F_{4,28}=24.3$, $p<0.001$), with the lowest mean value in Central Bay (11.9 ± 4.3 μM, $n=20$) and the greatest in South Bay (39.1 ± 7.4 μM, $n=4$; Fig. 2g, Supp. Table 1). Nitrate showed a distinct seasonal change: fall concentrations were lower (11.2 ± 3.3 μM, $n=19$) than winter (26.1 ± 10.2 μM, $n=14$; $t_{15.1}=5.2$, $p<0.001$; Fig. 2n). Nitrite concentrations were far lower than other nutrients: most samples were <1 μM, except for South Bay stations (4.8 ± 3.0 μM, $n=4$) and station USGS-24 at the southern end of Central Bay (1.1 μM; Supp. Table 1). Nitrite differed significantly between regions ($F_{4,28}=15.6$, $p<0.001$; Fig. 2f) but was only marginally different between fall (0.4 ± 0.3 μM, $n=19$) and winter (1.8 ± 2.4 μM, $n=14$; $t_{13.2}=2.1$, $p=0.052$; Fig. 2m).

SPM concentrations from the USGS database were linearly correlated to k_d ($r^2=0.837$, $p<0.001$) but not chlorophyll ($r^2=0.042$, $p=0.104$), and removing chlorophyll improved model performance. Therefore, k_d was the only variable used to model surface SPM (final model: $\mathrm{SPM}=\frac{k_d-0.340}{0.594}$). Comparing measured (database) and modeled surface SPM concentrations from *Polaris* cruises on September 15 and November 20, 2011 showed a highly significant linear correlation ($r^2=0.840$, $p<0.001$). We were therefore confident that this model reasonably estimated SPM concentrations in San Francisco Bay and used it to calculate surface SPM concentrations for *Questuary* stations, which were then propagated through the water column using the measured turbidity profiles from these stations. Modeled SPM values were relatively low (2.0 to 21.7 mg L^{-1}, $n=11$; Supp. Table 1). Overall, SPM varied both regionally ($F_{4,28}=3.4$, $p=0.022$) and temporally

($t_{23.2} = 4.6$, $p < 0.001$), with a total range from 2.0 to 176.0 mg L^{-1} (Supp. Table 1). Mean SPM was high in South Bay (30.7 ± 15.9 mg L^{-1}, $n = 4$) and North Bay (53.7 ± 81.6 mg L^{-1}, $n = 4$; Fig. 2d) and higher across all regions in winter (33.5 ± 43.3 mg L^{-1}, $n = 14$) than in fall (7.6 ± 5.4 mg L^{-1}, $n = 19$; Fig. 2k). At stations where more than one depth was sampled, SPM was often greater in bottom waters than surface waters (Supp. Table 1).

In the PCA of environmental data, the first two principle components explained 61.8 % of the environmental variance. Samples clustered distinctly by season, with October cleanly separated from December and February (Fig. 3). This clustering was driven largely by increased temperature and chlorophyll in October, as well as decreased nitrate, nitrite, and SPM concentrations.

Nitrification Rates

When $\delta^{15}N_{NOx}$ was measured ≥3 times over the incubation period, increases were linear over time ($r^2 = 0.994 \pm 0.006$, $n = 26$), including samples from all regions and across our range of measured rates. Therefore, the use of an endpoint model to calculate nitrification rates was justified. Nitrification was detected in all samples, with a minimum value of 6.6 nM day^{-1} at station SFQ-2 (Central Bay surface waters) and a maximum of 310.2 nM day^{-1} at station USGS-9 (North Bay bottom waters, in Carquinez Strait; Fig. 4). In general, nitrification rates were lowest in Central Bay (30.1 ± 25.1 nM day^{-1}, $n = 20$), particularly in waters closest to the Pacific Ocean. In regions further from the ocean, nitrification was generally higher but quite variable, with mean values of 75.8 nM day^{-1} (±80.3) in South Bay, 150.2 nM day^{-1} (±132.5) in North Bay, and 112.3 nM day^{-1} (±38.4) in the Sacramento River. This regional pattern was statistically significant ($F_{4,28} = 5.0$, $p = 0.003$). Nitrification did not vary significantly between seasons ($t_{20.8} = 1.5$, $p = 0.160$).

Linear Regression Models

Significant outliers were present in SPM and nitrite (Supp. Fig. 1). Nitrite concentrations were highest in South Bay, especially at station USGS-30 in December (Supp. Table 1), confirming previous reports of high concentrations of nitrite, as well as other nutrients (Wankel et al. 2006; Mosier and Francis 2008), in this region. The lone SPM outlier was station USGS-9 (Supp. Table 1) in Carquinez Strait, an area known to have transiently high bottom-water SPM due to sediment resuspension and trapping (Schoellhamer 2001). Therefore, outliers in both nitrite and SPM represent ecosystem variability and not measurement error. Log transformations of both variables resulted in a more even spread (Fig. 5) and were therefore used in all linear regression models. VIF analysis suggested numerous collinear variables (nitrite, nitrate, and salinity), which were sequentially removed from the initial model.

Fig. 2 Boxplots of environmental data, grouped by **a**–**g** region and **h**–**n** season. In **a**–**g**, *left* to *right* shows South Bay, Central Bay, North Bay, and the Sacramento River. For seasonal groupings, October cruises are designated as "fall," while December and February cruises are designated as "winter." In **h**–**n**, fall data is on the *left* and winter is on the *right*

The multiple linear regression model explaining the highest proportion of variance in nitrification rates included SPM, temperature, and ammonium as explanatory variables, with regression coefficients shown in Table 1. Nitrification was log transformed due to a pattern in the residual plot prior to transformation. Overall, the linear model explained 68 % of the variance in nitrification and was highly significant ($F_{3,29} = 23.8$, $p < 0.001$; Table 1). All three environmental variables were positively related to nitrification, with SPM and ammonium having the most significant effects. This model reflected the general pattern of high nitrification rates in samples with high SPM (USGS-30 and USGS-9 bottom waters) or high ammonium (USGS-30 and USGS-657). Since temperature varied seasonally across San Francisco Bay (Fig. 2i), it is interesting that while nitrification rates were not statistically different between seasons (see "Nitrification Rates" section), inclusion of temperature in the regression model with log SPM and ammonium increased the explanatory power, suggesting that there may be a relationship between nitrification and temperature when SPM and ammonium are also taken into account. There was no evidence of strong collinearity between temperature and either log SPM or ammonium (Fig. 5).

Discussion

Nitrification in San Francisco Bay: Regional Differences and Relationships with Ammonium and SPM

Although quantifying nutrient fluxes in estuaries is of paramount importance for understanding anthropogenic impacts on coastal ecosystems, biogeochemical rates of many processes remain understudied in many estuaries. To our knowledge, the data presented here are the first published water column nitrification rates from the San Francisco Bay ecosystem. Nitrification in this estuary showed high regional variation, with lower values close to the Pacific Ocean and higher values in either North Bay or South Bay. Different embayments within San Francisco Bay are physicochemically distinct, displaying variation in several environmental factors (Conomos et al. 1985; Kimmerer 2004) that could affect nitrification rates. Tidal exchange with the ocean leads to waters in Central Bay with shorter residence times, higher salinity, lower turbidity, and lower ammonium than other regions

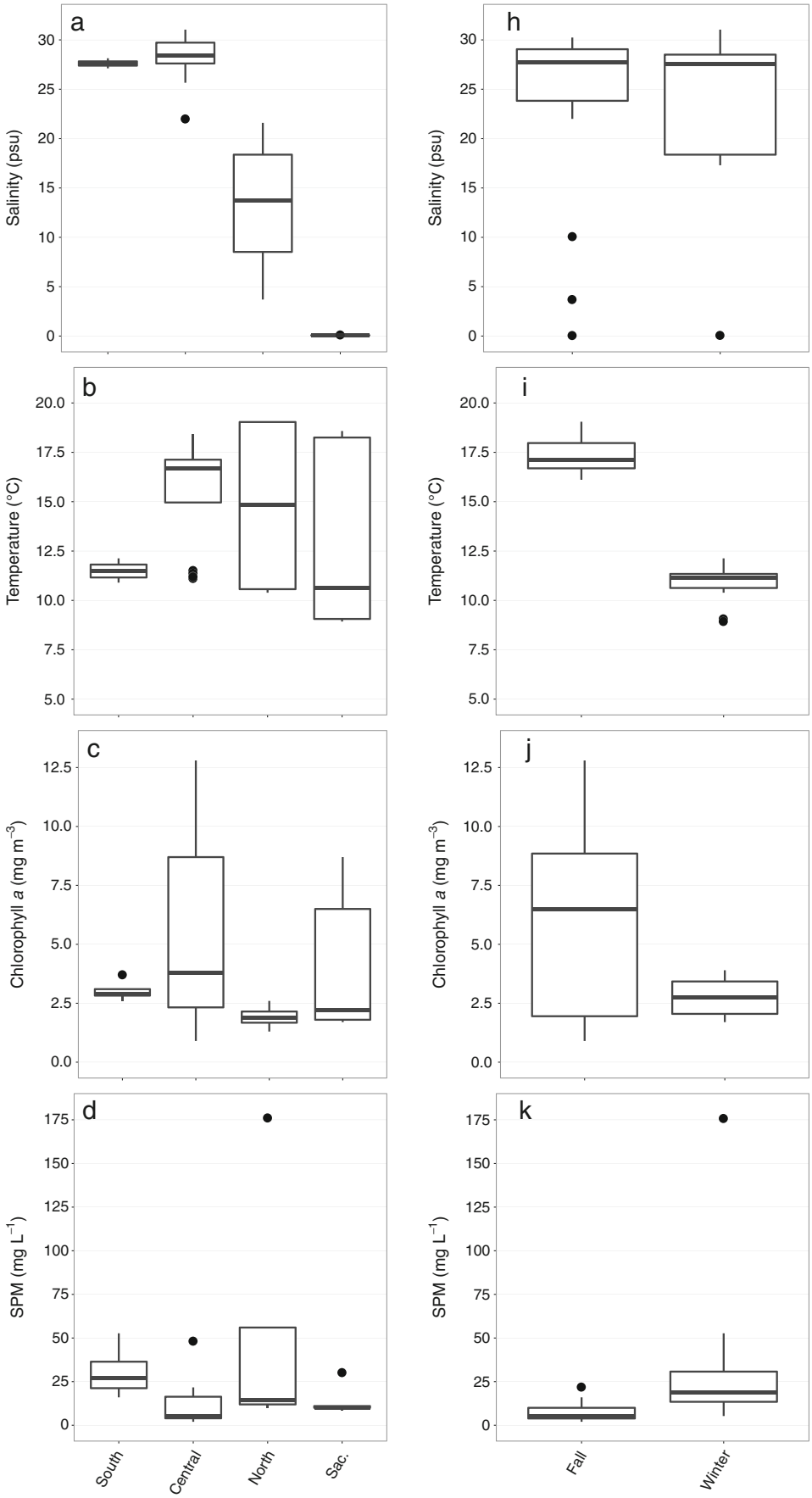
a
h
b
i
c
j
d
k
Salinity (psu)
Temperature (°C)
Chlorophyll a (mg m−3)
SPM (mg L−1)
South
Central
North
Sac.
Fall
Winter

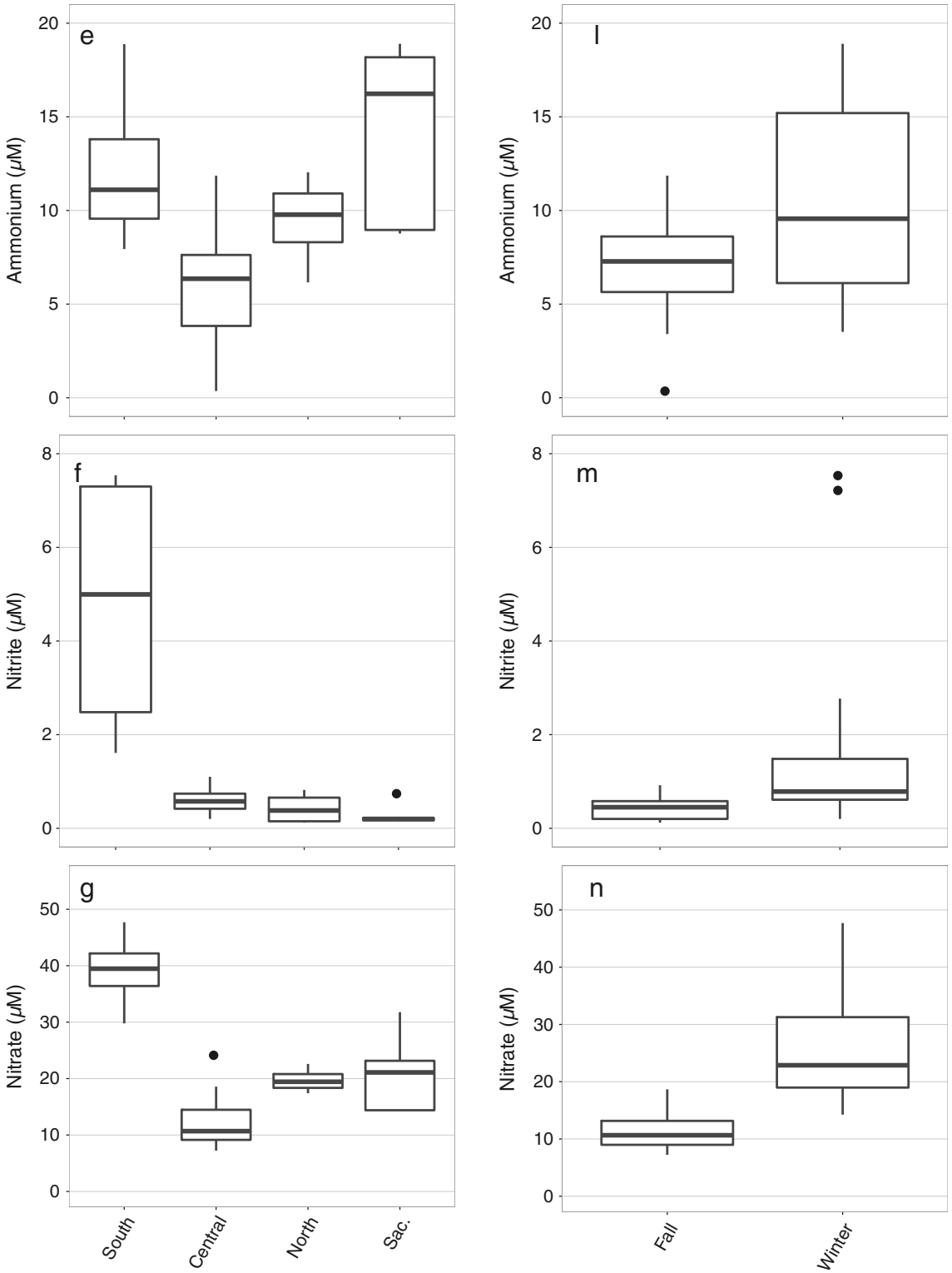

Fig. 2 (continued)

(Conomos et al. 1985; Walters et al. 1985; Kimmerer 2004). Therefore, though the Central Bay stations sampled here were quite diverse (for instance, station SFQ-2 is located in the deep channel just inside the Golden Gate, SFQ-4 is over a shoal, and USGS-13 is located in the channel of San Pablo Bay), most nitrification rates in this region were low (Fig. 4). Although our sampling effort in North Bay and the Sacramento River was limited, average nitrification rates in

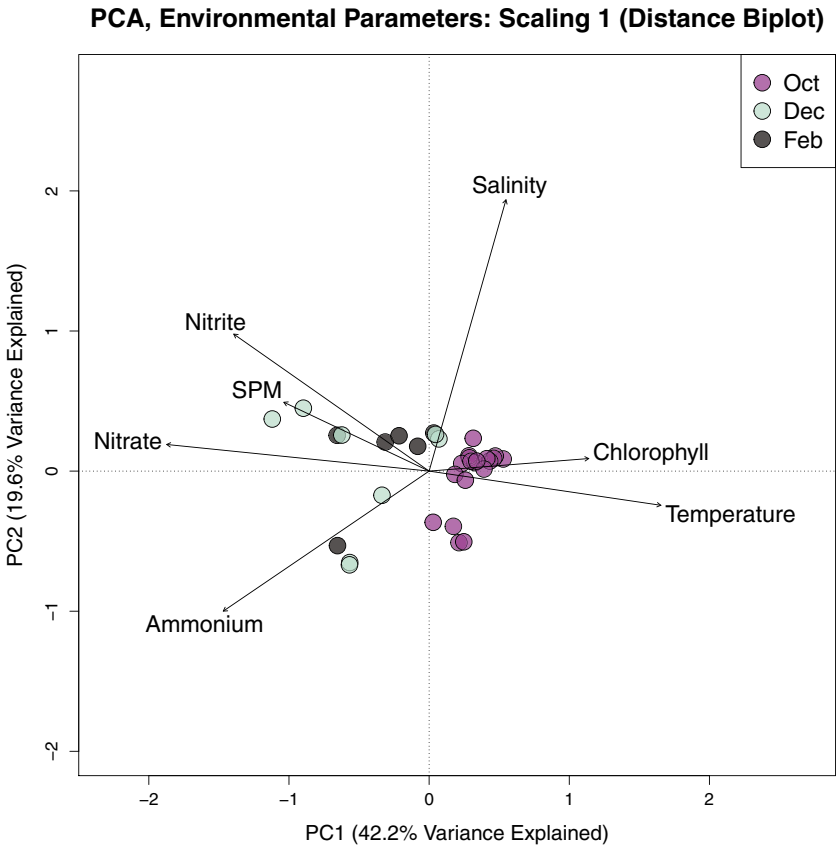

Fig. 3 Biplot representation of a PCA using transformed environmental data. The z-transformation was used to standardize across varying scales. Distances between points represent the Euclidean distances between samples in multidimensional space, and projections of a point onto a vector represent the position of a sample on that environmental parameter. Points are *colored* by month sampled

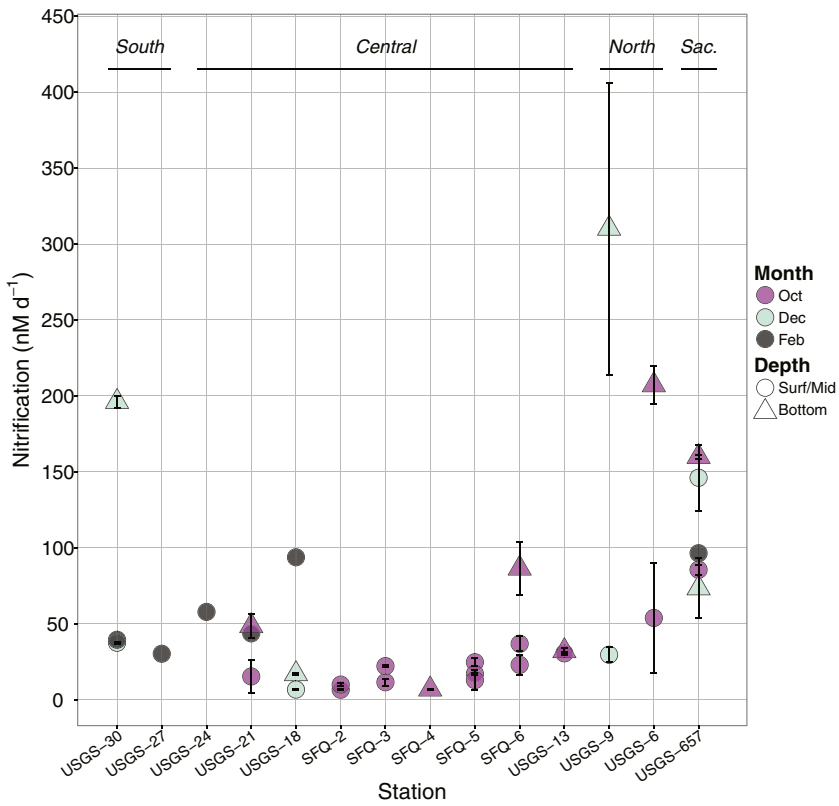

Fig. 4 Nitrification rates in San Francisco Bay waters. Samples are *colored* by month sampled. *Shapes* represent surface/mid-water vs. bottom-water samples. For samples with duplicate measurements taken, the *point* shows the midpoint and *error bars* show the range. Region is denoted at the *top of the figure* (*Sac.* Sacramento River)

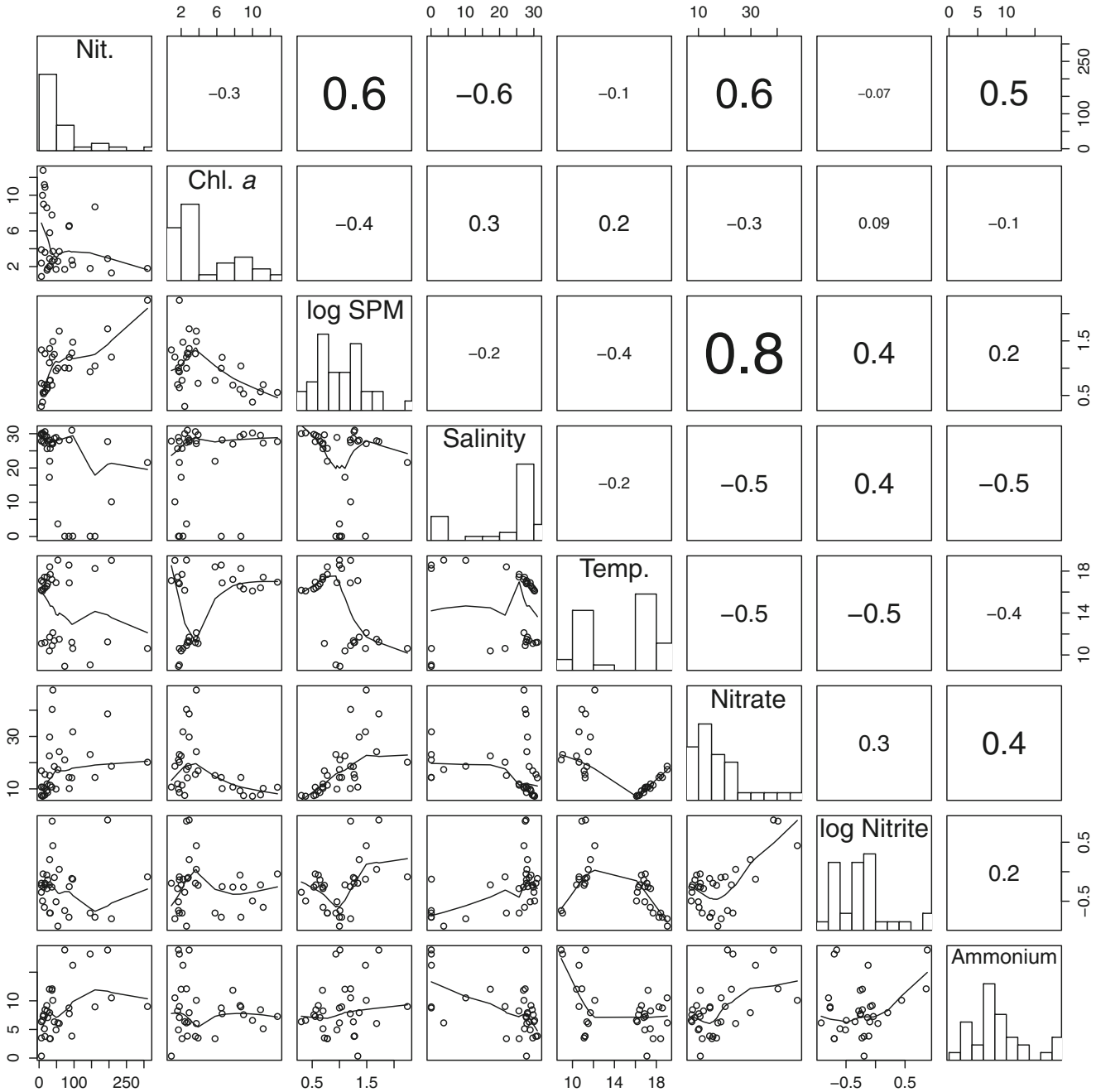

Fig. 5 Pairplots of environmental variables, to assess collinearity (see Zuur et al. 2009). *Plots below the diagonal* show scatterplots of each pairwise combination of variables, with a LOESS smoother. *Panels above the diagonal* show rank correlation coefficients (Spearman's ρ), with font size corresponding to strength of the correlation (only if the absolute value of Spearman's $\rho \geq 0.3$, for legibility). *Figures along the diagonal* show histograms for each variable

these regions were higher than those in Central Bay (particularly in bottom waters), reflecting a general increase in fresher, higher ammonium waters (Fig. 4; Table 1). Wastewater effluent discharged into the Sacramento River provides a constant and plentiful source of ammonium to the lower river and northern bay. While a significant fraction of the ammonium is depleted in the lower Sacramento River before reaching the estuary (Parker et al. 2012), enough effluent reaches the upper bay to increase ammonium concentrations substantially compared to waters further downstream (Fig. 2e). Additionally, turbidity in the low-salinity regions of San Francisco Bay is high enough to limit primary productivity (Cole and Cloern 1984; Alpine and Cloern 1988) and thus decrease light inhibition of nitrifiers (Horrigan and Springer 1990) or potential competition for ammonium between primary producers and nitrifiers (Smith et al. 2014a).

Table 1 Multiple linear regression parameters explaining log-transformed nitrification

Parameter	Estimate	Std. error	Partial r^2	t	p value
Intercept	−0.575	0.377			
log SPM	0.800	0.124	0.589	6.44	<0.001***
Temperature	0.058	0.017	0.282	3.37	0.002**
Ammonium	0.058	0.011	0.478	5.15	<0.001***
			$r^2 = 0.68$	$F_{3,29} = 23.8$	$p < 0.001$

Collinear explanatory variables were removed, based on VIF analysis and pairplots. For environmental variables, asterisks denote statistical significance of $^{**}p < 0.01$ and $^{***}p < 0.001$

In contrast to the northern regions of San Francisco Bay, South Bay (south of USGS-24; Fig. 1) has little freshwater input (Conomos et al. 1985; Kimmerer 2004). Tidal transport of water from Central Bay and mixing with wastewater effluent discharged into lower South Bay (the dominant source of freshwater to this region) create a well-mixed, polyhaline "lagoonal" ecosystem dominated by extensive shoals. The paucity of freshwater and the restriction of exchange with Central Bay lead to high water residence time in South Bay, typically on the order of months (Cheng and Gartner 1985; Walters et al. 1985). Long water residence times not only allow for remineralization of much of the organic matter in South Bay, but would also provide time for nitrifying populations to grow to substantial population sizes without being advected out of the estuary. Nutrient concentrations (particularly nitrate, but also ammonium and nitrite) are high due to inputs from treated wastewater (Cloern and Jassby 2012), and turbidity in this region is also relatively high due to wind stress over the shoals (see "Nitrification and SPM in San Francisco Bay" section below). The combination of long water residence time, tidal mixing, high turbidity, and relatively high productivity in this region results in high benthic remineralization and ammonium production (Caffrey 1995; Grenz et al. 2000), as well as high heterotrophic activity in bottom waters (Caffrey et al. 1998). Our data suggest that water column nitrification rates in this region are high, as well.

Throughout San Francisco Bay, nitrification rates generally paralleled concentrations of SPM (higher rates near the sediment-water interface or in more turbid regions of the bay) and ammonium (higher rates in the Sacramento River and South Bay), which were identified as having the strong effects on nitrification (Table 1). We discuss nitrification in San Francisco Bay in the context of these two environmental variables below.

Nitrification and SPM in San Francisco Bay

In most regions of San Francisco Bay, local SPM dynamics are driven by a combination of resuspension and advection between shoals and channels, while system-wide dynamics largely depend on sediment delivered via riverine pulses. Our data showed a correlation between nitrification rates and SPM concentrations across all regions in San Francisco Bay (Spearman's $\rho = 0.63$, $p < 0.001$), suggesting that it is a robust feature of this ecosystem. Even discounting USGS-9 bottom waters (a high outlier for both SPM and nitrification), this correlation was still significant (Spearman's $\rho = 0.59$, $p < 0.001$). Many river-dominated estuaries have large estuarine turbidity maxima (ETMs) in low-salinity regions, where particles are trapped in bottom waters (Jay and Musiak 1994). ETMs in San Francisco Bay mainly occur due to effects of bathymetry and sediment resuspension and are therefore typically restricted to fixed locations (e.g., near sills) rather than specific salinities (Schoellhamer 2001; Ganju and Schoellhamer 2008), though SPM concentrations are generally higher in brackish North Bay waters compared to both riverine and marine regions (Conomos et al. 1985; Hollibaugh and Wong 1999). Turbidity is also high in South Bay (south of station USGS-24), which consists primarily of broad shoals where sediment is easily resuspended by wind and wave action and then advected to the channel during ebb tides (Schoellhamer 1996; Brand et al. 2010). North Bay and Central Bay also have numerous shallow regions (e.g., San Pablo Bay and Grizzly Bay) where wind and wave resuspension can be strong and lead to short-time variations in SPM (Ruhl et al. 2001; Warner et al. 2004). However, SPM fluctuations throughout the northern estuary over seasonal time scales are strongly influenced by sediment-rich freshwater pulses in winter and spring (Ruhl and Schoellhamer 2004; McKee et al. 2006).

Previous work showed roughly one third of the microbial abundance and activity in northern San Francisco Bay waters is particle-associated, particularly following sediment delivery from the rivers in spring and early summer (Hollibaugh and Wong 1999; Murrell et al. 1999). Even during low-flow conditions when microbial populations throughout the estuary are generally smaller and less active (likely due to decreased organic matter delivery from the rivers), particle-associated microbial activity remains high in brackish waters compared to riverine and marine regions, in parallel with higher SPM in brackish regions (Hollibaugh and Wong 1999). The correlation between nitrification and SPM suggests that nitrifiers may be particularly active on particles, as well. Notably, while Central Bay had the lowest nitrification rates, two samples (from stations USGS-18 and SFQ-6) had relatively high nitrification rates for this region. Surface water nitrification at station USGS-18 increased dramatically between December 2011 and February 2012, from 6.6 to 93.7 nM day^{-1} (Fig. 4), in parallel with a considerable increase in SPM (Supp. Table 1). The February cruise was preceded by a spike in Delta outflow (greater than 875 m^3 s^{-1}) due to a rainstorm in late January 2012 (Supp. Fig. 2), which likely transported sediment from the Delta to Central Bay (e.g., McKee et al. 2006). While higher resolution seasonal sampling is needed to

fully assess the effects of freshwater discharge on nitrification, the data from Central Bay stations corroborate the idea that biogeochemical cycling throughout San Francisco Bay is enhanced after periods of high freshwater discharge.

Correlations between nitrification and SPM may be due either to the suspension of active ammonia oxidizers from surface sediments or to increases in ammonium delivered from the sediments to the water column. Our data establishes correlative evidence of an association between these factors but cannot yet determine the ultimate cause of this relationship. Previous work has documented abundant populations of AOA and AOB in surface sediments throughout San Francisco Bay (Mosier and Francis 2008; Damashek et al. 2015), but it is not known whether the ammonia-oxidizing communities in the water column are similar to benthic communities. Nitrifying microbes are known to associate with estuarine particles in many systems, increasing nitrification rates in ETMs: for instance, numerous studies have suggested that nitrifiers in surface sediments are numerous but oxygen-limited until resuspension of microbial populations (along with sediments) into the oxic water column in an ETM stimulates these dense populations and leads to high nitrification rates, similar to a "fluidized bed reactor" (Helder and De Vries 1983; Owens 1986). If this mechanism holds true in San Francisco Bay, we expect the active nitrifying communities in turbid bottom waters to contain clades commonly found in surface sediment communities that have been stimulated via resuspension into the oxygen-rich water column.

Nitrification and Ammonium in San Francisco Bay

Nitrification rates in San Francisco Bay were strongly influenced by ammonium concentrations (Table 1), which exceeded 5 μM at most stations (Supp. Table 1). San Francisco Bay receives ammonium from a myriad of sources, with high ammonium in the Sacramento River and North Bay primarily due to the discharge of treated wastewater from the Sacramento Regional Wastewater Treatment Plant (Jassby 2008). Similarly, wastewater effluent from the San José-Santa Clara Regional Wastewater facility may contribute to elevated ammonium in South Bay, as a fraction of effluent from this facility is ammonium (Yigzaw 2014). Both of these regions could be conducive to hosting abundant nitrifying microbial populations: in addition to constantly high ammonium concentrations, South Bay has long water residence times, and the lower Sacramento River is far enough downstream of the sewage outfall to allow for substantial population growth by the time that the ammonium-rich water reaches this point. It is worth noting that our Sacramento River station had much lower ammonium concentrations than is typical of sites further upstream (e.g., Parker et al. 2012); nitrification rates at upstream sites with higher ammonium concentrations remain unknown.

In addition to housing robust microbial communities (as discussed above), estuary sediments are massive repositories of ammonium, as limitation of available oxidants allows ammonium and other reduced ions to accumulate in anoxic sediment layers (Jørgensen et al. 1990). Multiple studies have documented porewater ammonium concentrations in San Francisco Bay sediments exceeding 100 μM near the sediment-water interface (Hammond et al. 1985; Rivera-Duarte and Flegal 1994; Caffrey 1995). As surface sediments are resuspended, this porewater ammonium may be liberated into the water column. Additionally, there could also be ammonium desorbing from the resuspended particles themselves: due to their positive charge, ammonium ions can be adsorbed to negatively charged sites on sediment particles, but as sediments are resuspended into the water column, ionic interactions promote desorption of ammonium. Desorption can lead to a rapid ammonium pulse into the water and can be capable of contributing as much ammonium to the water column as diffusive sediment-water efflux (Simon 1989; Morin and Morse 1999; Fitzsimons et al. 2006). For example, recent data from the Great Bay Estuary (New Hampshire, USA) showed increases in ammonium concentrations in bottom waters during periods of high bed shear stress, exceeding concentrations expected from porewater resuspension alone (Percuoco et al. 2015; Wengrove et al. 2015). Our data did not show a correlation between SPM and ammonium (Spearman's $\rho = 0.169$, $p = 0.348$). However, if increased ammonium availability stimulates bottom water nitrification or other ammonium-consuming processes, liberated ammonium may be oxidized or assimilated rapidly enough to obscure the relationship between ammonium and SPM.

Context of Nitrification in San Francisco Bay

Nitrification rates in San Francisco Bay waters showed a fairly wide range, including many measurements greater than 50 nM day^{-1}, which is typical open marine waters (e.g., Ward et al. 1982; Dore and Karl 1996; Newell et al. 2013) and comparable to higher rates occasionally reported from the lower euphotic zone or oxic/anoxic transition layers in the sea (Beman et al. 2008; Lam et al. 2009; Santoro et al. 2010; Smith et al. 2015). However, while this study focused on the spatial characterization of nitrification in San Francisco Bay, samples were only collected during the fall and winter of 1 year, and many stations were only sampled once. Thus, there may be temporal variability in nitrification rates within each region of this ecosystem that we were unable to capture with our current sampling effort.

To further understand nitrification in San Francisco Bay as compared to other estuaries, we compiled pelagic nitrification rates from the estuarine literature (Table 2). A wide range of methods have historically been used to measure nitrification in estuary waters, and rates measured using disparate techniques

Table 2 Estuarine nitrification rates from the primary literature

Estuary	Classification	Method	Rates[a] (nM day^{-1})	NH_4^+ (μM)	NO_3^- (μM)	NO_2^- (μM)	Salinity	SPM (mg L^{-1})	Patterns/correlations	Reference
Baltic	Stratified brackish inland sea	^{15}N, ^{14}C + N-serve	1–280	0.2–2	0–6	0–0.2	7.0–11.0	NA	O_2 (−); high at halocline	Enoksson (1986)
Baltic	Stratified brackish inland sea	^{15}N, denitrifier method	3.2–83.6	0.7–17.0	0–7.66	0–0.67	8.9–12.4	NA	O_2 (−)	Hietanen et al. (2012)
Chang Jiang	River plume	^{15}N, denitrifier method	0–4600	0–2.0	0–149	0–1.0	0.2–34.3	2.6–3000	NH_4^+ (+); SPM (+)	Hsiao et al. (2014)
Chesapeake	Seasonally stratified estuary	^{15}N, azo dye method	170–1700	0.01–1.1	3.5–9.6	0–3.6	NA	NA	O_2 (−); NH_4^+ (+); high at pycnocline	McCarthy et al. (1984)
Chesapeake	Seasonally stratified estuary	^{15}N, azo dye method	72–83,064	0–30	1–60	0–4	11–16.5	NA	NH_4^+ (+); high at pycnocline	Horrigan et al. (1990)
Delaware	Well-mixed estuary	^{15}N, azo dye method	21–581	1–43	100–200	1–25	NA	NA	NH_4^+ (+); high below wastewater input	Lipschultz et al. (1986)
Hood Canal	Seasonally stratified fjord	^{15}N, azide method	11–417	0.01–7.03	2–50	0–5	24.6–30.7	NA	NH_4^+ (−); NO_3^- (+); high below pycnocline	Urakawa et al. (2014)
Hood Canal	Seasonally stratified fjord	^{15}N, azide method	0–316	0–0.7	0–35	0–0.4	23–30	NA	Higher below pycnocline	Jacquot et al. (2014)
Hood Canal	Seasonally stratified fjord	^{15}N, azide method	0–550	0–0.7	0–30	0–0.4	26.5–30	NA	High below pycnocline and primary NH_4^+ max.	Horak et al. (2013)
Long Island Sound	Well-mixed estuary	^{13}N	1800–7056	1.0–6.0	NA	NA	NA	NA	NH_4^+ (+)	Capone et al. (1990)
Mississippi	River plume, stratified coastal sea	^{15}N, azide method/sulfamic acid	9–494	0–0.72	0.1–11.4	0–4.6	27–36	NA	O_2 (−); NO_2^- (+)	Bristow et al. (2015)
Mississippi	River plume, stratified coastal sea	^{15}N-NO_X isotope dilution	9–3500	1.0–2.5	0.5–3.5[c]	NA[c]	23–34	NA	NO_X (+)	Carini et al. (2010)
Mississippi	River plume, stratified coastal sea	Nutrients	0–13,440	0.8–2.4	3.4–114.3	0.01–1.56	0–36.0	NA	High at intermediate salinity	Pakulski et al. (1995)
Mississippi, Atchafalaya	River plume, stratified coastal sea	Nutrients	0–14,160	0.5–2.5	0–200	0–2.5	0–35	NA	Chl. (−); bacterial abund. (−); Salinity (−)	Pakulski et al. (2000)
Narragansett	Well-mixed estuary	^{14}C + N-serve	10–11,200	0–82	0–178[c]	0.1–4	0–33	NA	Temperature (+); NH_4^+ (+)	Berounsky and Nixon (1993)
Narragansett	Well-mixed estuary	^{14}C + N-serve	Up to 11,000	43.6–43.9[d]	24.5–43.9[cd]	NA[c]	20.5–25.5[d]	NA	Temperature (+)	Berounsky and Nixon (1990)
Narragensett (lower)	Well-mixed estuary	Nutrients (no-addition mesocosms)	Up to 550	1–4	0–9[c]	0.2–0.8	28–32	NA	NH_4^+ (+)	Berounsky and Nixon (1985)
Nervión	Stratified river-dominated estuary	^{14}C + N-serve	0–14,760	0–43	0–16	0.1–7	0.1–35.7	4.2–181.2	O_2 (−); temperature (+); salinity (−)	Iriarte et al. (1998)
North Sea	Well-mixed coastal sea	^{15}N, Devarda's alloy/diffusion	984–5304	1.5–10	5–80	0.25–2	20–32	NA	Sporatically high in late fall, early spring	Veuger et al. (2013); Pitcher et al. (2011)
Pearl	Seasonally stratified river-dominated estuary	Nutrients + ATU	0–33,100	1.2–832.1	16.7–266.2	4.0–67.8	0–34	16.2–51.2	Temperature (+); O_2 (−)	Dai et al. (2008)
Plymouth Sound	Well-mixed coastal sea	Nutrients + ATU (control-pH treatment)	55–60	NA	NA	NA	NA	NA	pH (+)	Kitidis et al. (2011)
Rhône	River plume	Nutrients + ATU, ^{14}C + ATU	230–2150	1.0–9.8	2.6–112.8	0.4–3.9	0–37	9.8–22.6	Salinity (−); NH_4^+ (+); NO_2^- (+); NO_3^- (+); SPM (+)	Feliatra and Bianchi (1993)
Rhône	River plume	Nutrients + N-serve	230–2200	0–10	0–10	0–2.5	7–35	NA	Salinity (−); NH_4^+ (+); NO_2^- (+); NO_3^- (+)	Bianchi et al. (1994)
Rhône	River plume	Nutrients + ATU, ^{14}C + ATU	120–4200	0.5–11	0.5–130	0.2–5	7–37	22.6–38.9[d]	Salinity (−); temperature (+); SPM (+)	Bianchi et al. (1999)
Saanich Inlet	Seasonally stratified fjord	Nutrients + ATU	0–7656	0–4.9	0–28.9	0.02–1.1	28.5–31	NA	NO_2^- (+)	Grundle and Juniper (2011)
Saanich Inlet	Seasonally stratified fjord	^{15}N, azo dye method	10–120	0.1–3.5	0–30	0–0.25	NA	NA	Low beneath oxic/anoxic interface, one high rate at interface	Ward and Kilpatrick (1990)
Sapelo Island	Salt marsh-dominated well-mixed estuary	^{15}N, denitrifier method	0.9–804	0.1–6.5	0.9–5.9	0.05–7.1	NA	NA	Temperature (+); high during flood tide	Tolar (2014)
Scheldt	Well-mixed estuary	^{14}C + unknown inhibitor	0–24,000	10–1400	0–250	NA	0–18	NA	NH_4^+ (+); temperature (+); O_2 (−)	Somville (1978)
Scheldt	Well-mixed estuary	^{14}C + N-serve	Up to 80,000	10–750	0–225	NA	0.7–27	NA	High in low-salinity region	Somville (1984)

Table 2 (continued)

Estuary	Classification	Method	Rates[a] (nM day^{-1})	NH_4^+ (μM)	NO_3^- (μM)	NO_2^- (μM)	Salinity	SPM (mg L^{-1})	Patterns/correlations	Reference
Scheldt	Well-mixed estuary	^{14}C + methylfluoride, nutrients	Up to 153,600	0–400	125–400	NA	0–33	NA	Salinity (−); NH_4^+ (+); O_2 (−)	de Wilde and de Bie (2000)
Scheldt	Well-mixed estuary	^{14}C + N-serve	Up to 4500	5–500	NA	NA	0–16	15–300	High in low-salinity region in summer	de Bie et al. (2002)
Scheldt	Well-mixed estuary	O_2 + N-serve	0–18,260	0–125[d]	75–375[cd]	NA[c]	0–28	NA	Salinity (−); NH_4^+ (+); temperature (+)	Gazeau et al. (2005)
Scheldt	Well-mixed estuary	^{15}N, Devarda's alloy/diffusion	0–16,836	0–150	25–450[c]	NA[c]	0–30	10–250	Salinity (−); NH_4^+ (+); SPM (+)	Andersson et al. (2006)
Scheldt	Well-mixed estuary	^{15}N, Devarda's alloy/diffusion	Up to 14,400	0–150	25–450[c]	NA[c]	0–30	NA	Salinity (−); NH_4^+ (+)	Brion et al. (2008)
Seine	Partially mixed estuary	^{14}C + N-serve	0–33,600	0–350	200–500[c]	NA[c]	0–13	10–2000	SPM (+)	Brion et al. (2000)
San Francisco Bay	Well-mixed estuary	^{15}N, denitrifier method	7–310	0.4–19	7.2–47.7	0.1–7.5	0.1–31	2–176	SPM (+); NH_4^+ (+); salinity (−)	This study
Tamar	Partially mixed estuary	^{14}C + N-serve	0–4000	2–20	5–120	0–3	0–30	1–420	SPM (+); salinity (−)	Owens (1986)
Urdaibai	Well-mixed estuary	^{14}C + ATU	0–4610	75–375	10–80	1–3	0–34	NA	SPM (+)[e]; salinity (−)	Iriarte et al. (1996)
West Florida Shelf	Well-mixed coastal sea and adjacent estuaries	^{15}N, denitrifier method	888–6120	0.5–1.5[d]	0.1–0.5[d]	NA	NA	NA	High at sites with high productivity and NH_4^+ regeneration	Bronk et al. (2014)
Baltic	Stratified brackish inland sea	^{15}N, cadmium reduction/sulfamic acid	0.2–884[b]	0.1–13.6	0–8.0	0.1–0.4	NA	NA	NO_2^- (+); O_2 (−) not including hypoxic waters	Berg et al. (2015)
Gironde	Partially mixed estuary	Nutrients + N-serve (fluid mud slurries)	264,000–336,000[b]	1–15	10–150	0–13	0–32	0–450,000	High at low-salinity sites	Abril et al. (2000)
Kochi	Well-mixed monsoonal estuary	^{15}N, azo dye method	1–3984[b]	0–110	0–70	0–1	0–35	NA	Temperature (+); NH_4^+ (+); high at intermediate salinities	Miranda et al. (2008)
Sagami	Well-mixed coastal sea	^{15}N, azo dye method	0.3–8.6[bf]	0.02–0.1	0–0.6	0.01–0.03	NA	NA	High below thermocline	Miyazaki et al. (1973)
Seine	Partially mixed estuary	^{14}C + N-serve	14,400–62,400[b]	0–250	215–500	NA	NA	NA	High at low-salinity sites	Cébron et al. (2003)

Only data from bottle incubations are included. Data from rivers are included only if they include portions of an estuary (salinity gradients or tidal influence). Coastal ocean data are reported only if the region was strongly influenced by an estuary or river plume (decreased salinity or elevated nutrients). Reported patterns and correlations only consider environmental factors (and not factors such as microbial abundance or diversity). Data are estimated from figures when exact values were not reported

[a] All reported rates were converted to nanomolar per day. Data reported in molar carbon units were converted to molar nitrogen units using the ratio of 8.3 mol carbon fixed per 1 mol of ammonia oxidized (Somville 1978), as this was a commonly used conversion factor in the literature

[b] Potential rate measurements, which likely overestimate in situ rates

[c] Reported as nitrate + nitrite

[d] Nutrients reported only as average values

[e] Relation to SPM inferred from light extinction coefficient data

[f] Rates reported in text as microgram atoms N per liter per hour and in tables as nanogram atoms N per liter per hour. Here, rates were converted using the former units, as the latter produced extremely low rates, and nutrient concentrations throughout Miyazaki et al. (1973) were reported in the former

may not always be directly comparable. In particular, many previous studies estimated nitrification rates indirectly by measuring dark carbon fixation in parallel incubations with and without nitrification inhibitors, typically either 2-chloro-6-trichloromethyl pyridine ("N-serve") or allylthiourea (ATU; Table 2). While these measurements provide an estimate of active nitrifier growth, they may not be directly comparable to rates measured using ^{15}N tracers, for numerous reasons. First, the ratio of ammonia oxidized to carbon fixed can vary substantially in both laboratory cultures and environmental populations of ammonia oxidizers (Andersson et al. 2006). Second, carbon-based methods assume that all nitrifiers in an incubation grow autotrophically, but it is still debated whether some ammonia oxidizers (including some commonly found in estuaries) can grow mixotrophically (Ouverney and Fuhrman 2000; Hallam et al. 2006; Tourna et al. 2011). Finally, nitrification inhibitors used with this method were mostly chosen based on their effects on cultured AOB or soil nitrification rates (Lees 1952; Goring 1962; Ginestet et al. 1998), but their inhibition efficiency on ammonia-oxidizing archaea or naturally occurring populations of largely uncultivated organisms is not always clear (Hatzenpichler et al. 2008; Santoro et al. 2010; Jäntti et al. 2013). For these reasons, the following discussion avoids quantitative comparison between studies using dark carbon fixation and those using ^{15}N to measure nitrification rates, though both methods are useful ways to compare qualitative trends in nitrification within or between estuaries. We assume that both methods are comparable for large differences in rates (i.e., different orders of magnitude).

Nitrification in most estuaries is higher than in typical marine waters (Table 2), suggesting that estuary waters may be nitrification "hotspots," at least compared to most regions of the ocean. However, there is significant variability in the maximum nitrification rate between estuaries. Along with the data from San Francisco Bay reported here, rates measured in numerous estuaries (including Hood Canal, Sapelo Island, and the Baltic Sea) were greater than 50 nM day^{-1} but did not exceed 1000 nM day^{-1}, while those from other estuaries (the Scheldt estuary, Narragansett Bay, and Chesapeake Bay) were orders of magnitude higher (Table 2), with many reported rates exceeding 10,000 nM day^{-1}. Estuaries are notoriously complex ecosystems, so the documented variability between ecosystems is not surprising but warrants further investigation. The following discussion reflects on comparisons of nitrification rates between estuaries in relation to nutrients, SPM, and temperature, as these parameters have significant effects on nitrification in San Francisco Bay (Table 1). Other environmental factors are undoubtedly important in shaping estuarine nitrification rates: for example, pH and primary productivity are major factors affecting nitrification rates in estuarine and coastal ecosystems (Fulweiler et al. 2011; Smith et al. 2014a). Unfortunately, the paucity of studies measuring these parameters alongside nitrification rates in estuary waters precluded their inclusion.

Nitrification in Eutrophic Versus Oligotrophic Estuaries

In many eutrophic estuaries, nitrification was highest in waters with high ammonium concentration. Many estuaries receiving ammonium-rich wastewater effluent had high nitrification rates downstream of inputs (e.g., Somville 1984; Lipschultz et al. 1986; Iriarte et al. 1996; Brion et al. 2000), though there was often a separation between ammonium and nitrification maxima (e.g., Somville 1978; Brion et al. 2000). This gap is likely due to the time needed for the nitrifying populations to grow to a high density or, in some systems, to ventilate anoxic waters. Our data showing higher nitrification rates in South San Francisco Bay and the Sacramento River (Fig. 4) also match this pattern (see "Nitrification and Ammonium in San Francisco Bay" section). Comparison between estuaries shows that nitrification rates often reflect the ammonium loading of an ecosystem, as many of the highest nitrification rates were from estuaries with abundant ammonium (often exceeding 100 μM), while lower rates (<1000 nM day^{-1}) were reported in ecosystems with lower ammonium concentrations (Table 2). In this regard, the Scheldt estuary presents a unique case in studying nitrification in eutrophic estuary waters, as nitrification has been studied here for decades (Table 2) while nutrient inputs into the estuary have decreased significantly due to increased regulation (Soetaert et al. 2006). Even despite seasonal biases in sample collection, the unique data set from the Scheldt shows a clear trend of declining nitrification rates in recent years, concurrent with reduced ammonium concentrations (Table 2). Judging by the data from the Scheldt, nitrification rates in other estuaries with high ammonium loading may decrease if ammonium inputs are lessened.

While many sites with high nitrification rates had high ammonium concentrations, high rates (over 1000 nM day^{-1}) have also been reported in numerous lower-ammonium river plume or coastal shelf ecosystems (the West Florida Shelf, the coastal North Sea, and the Chang Jiang, Mississippi, and Rhône River plumes; Table 2). Over the West Florida Shelf, nitrogen mineralization and uptake were also high in the estuarine waters with highest nitrification rates (Tampa Bay and Charlotte Harbor), suggesting a link between nitrification and rapid ammonium cycling in highly productive surface waters (Bronk et al. 2014). The Mississippi and Chang Jiang plumes also had high nitrification rates and low ammonium concentrations (Pakulski et al. 1995, 2000; Carini et al. 2010; Hsiao et al. 2014; Bristow et al. 2015), while the Rhône plume had high nitrification rates in the ammonium-rich inner waters closest to the river (Feliatra and Bianchi 1993; Bianchi et al. 1994, 1999). Ammonium production can also be elevated in turbid river plumes (Pakulski et al. 1995, 2000), suggesting that high nitrification rates in these waters could be fed by high

ammonium production rates. In waters with strongly coupled ammonium production and oxidation, ammonia-oxidizing microbes may be adapted to rapidly scavenge and oxidize ammonium as it becomes available, leading to high nitrification rates but little ammonium buildup. Along these lines, recent evidence from Hood Canal showed that the Michaelis constant (K_m) of nitrification was less that 0.1 μM NH_4^+ (Horak et al. 2013), suggesting that the ammonia-oxidizing community here can respond to low ammonium concentrations. Tight coupling between ammonium production and oxidation may complicate efforts to compare ammonium concentration and nitrification between estuaries.

Additionally, there may be salinity-induced dynamics in nitrifying populations preventing rapid utilization of ammonium in low-salinity zones. Microbial population abundance in San Francisco Bay waters decreases in low-salinity mixing zones compared to freshwater regions (Hollibaugh and Wong 1999). Therefore, nitrifying populations in freshwater likely also decrease in abundance between the rivers into the upper estuary. Due to the relatively slow growth rates of nitrifiers (e.g., Santoro and Casciotti 2011; Mosier et al. 2012), it may take low-salinity communities on the order of days to grow to substantial population sizes, but by this point (depending on freshwater flow and circulation), mixing-induced salinity changes may favor a more halotolerant community. Thus, constant estuarine mixing patterns may continually dilute slow-growing nitrifying populations as water travels seaward, keeping their activity relatively low until they reach a body of water with a long enough residence time at a single salinity to grow to a substantial population size. Similarly, marine nitrifiers (typically adapted to high salinity, low-ammonium environments) advected into the estuary may not be present at large enough population sizes and may face similar salinity stress and thus be unable to rapidly oxidize available ammonium. Clearly, relationships between the population structure of nitrifying microbes, nitrification rates, and environmental parameters (including water residence time) are needed to clarify how these populations respond to environmental changes across the mixing gradients of the estuaries.

In theory, because nitrification produces nitrite and nitrate, nitrification rates should be correlated with their concentrations, but the studies summarized in Table 2 suggest that this is rarely the case. Nitrate dynamics in estuaries differ significantly between systems, with nearly conservative mixing in some estuaries and rapid nitrate uptake and turnover in others (Middelburg and Nieuwenhuize 2001; Wilkerson et al. 2006). Nitrite is rapidly oxidized or assimilated in estuaries and marine waters (McCarthy et al. 1984; Horrigan et al. 1990) and is therefore a very short-lived species, masking potential correlations between nitrite production and concentration. Therefore, while correlations between nitrification rates and nitrate or nitrite are occasionally documented (Table 2), rapid cycling by processes other than ammonia oxidation or mixing between water masses often obscures these relationships.

Nitrification in Turbid and Warm Estuary Waters

The strongest correlation with San Francisco Bay nitrification rates was SPM (Table 1), and nitrification in numerous other estuaries peaked in turbid, low-salinity waters near the benthos (Owens 1986; Berounsky and Nixon 1993; Iriarte et al. 1996; Brion et al. 2000; de Wilde and de Bie 2000; Pakulski et al. 2000; Hsiao et al. 2014). ETMs are often hotspots for heterotrophic activity and biogeochemical cycling (Goosen et al. 1999; Lee et al. 2012), and our rates add to the wealth of data showing enhanced nitrification in these regions. These include estuaries with ETMs in low-salinity regions (the Scheldt, Seine, and Tamar) as well as river plumes, which typically contain abundant allochthonous sediment (Benner and Opsahl 2001). While this correlation is strongly supported across diverse estuaries and has been documented for decades (e.g., Owens 1986; Feliatra and Bianchi 1993; Brion et al. 2000), further research is needed to clarify the mechanistic contributions of factors such as resuspension of microbes, ammonium desorption, and porewater ammonium resuspension in different ecosystems (see "Nitrification and SPM in San Francisco Bay" section). In addition to SPM and ammonium, temperature had a significant positive effect on nitrification rates in San Francisco Bay (Table 1), though the lack of data from spring and summer precludes a thorough analysis of seasonal aspects of nitrification in this system. Temperature was also positively correlated with nitrification rates in many estuaries (Table 2). Contrasting patterns between estuaries, however, suggest that nitrifying communities in various ecosystems respond to temperature differently (Table 2): in some regions, activity was highest in summer (Berounsky and Nixon 1990; Iriarte et al. 1998; Hollibaugh et al. 2014; Tolar 2014), while other regions had nitrification rates that peaked in winter (Baer et al. 2014) or were unresponsive to temperature (Horak et al. 2013). Therefore, a cross-system understanding of the effects of temperature on estuarine nitrification rates remains elusive.

Potential Dark Bottle Bias of Nitrification Measurements

A potentially important driver of nitrification in any pelagic ecosystem is light. For example, nitrification rates in the upper ocean and typically low in surface waters but increase at the base of the photic zone (Ward et al. 1982; Dore and Karl 1996; Santoro et al. 2010). Some studies suggest direct physiological inhibition of ammonia oxidizers by light (Horrigan and Springer 1990; Merbt et al. 2012), while others implicate competition between phytoplankton and ammonia oxidizers for available ammonium (Smith et al. 2014a). Because incubating water in dark bottles avoids any direct inhibitory effects on

ammonia oxidizers and inhibits photosynthetic ammonium uptake, nitrification rates from relatively clear surface waters measured in dark bottles may be overestimates of in situ rates.

Irrespective of its ultimate cause, light inhibition of nitrification should be minimal in relatively turbid, well-mixed estuaries such as San Francisco Bay. Photic zones in these systems are typically shallow, encompassing only a fraction of the total water column depth; indeed, low light availability in San Francisco Bay is commonly thought to limit phytoplankton growth (Alpine and Cloern 1988). Conversely, these conditions should *minimize* light inhibition of nitrification, as nitrifying populations in surface waters are rapidly mixed below the photic zone. Photic zone depth (Z_P) can be calculated as $Z_P = 4.61/k_d$, assuming that the depth of the photic zone extends from the surface to the depth of 1 % light penetration (Cloern 1987). Unfortunately, light attenuation (k_d) was not measured for many of our samples, including all samples from South Bay. For the data that we did collect, average Z_P for Central Bay stations was 6.85 ± 1.50 m ($n = 7$), while the lone stations from North Bay and the Sacramento River with light attenuation data had Z_P equal to 4.27 and 4.35 m, respectively. Therefore, our nitrification measurements may be slight overestimates in Central Bay surface waters, which are relatively clear compared to the rest of the bay, and in shoal stations, where the Z_P is a larger fraction of total water column depth. However, data from this study does not yet allow for an estimate of the magnitude of this bias in San Francisco Bay, as most of our sampled stations were in the estuary channel.

Rate Calculation Assumptions

One of the unknowns in our nitrification calculations is the initial isotopic value of ammonium ($\delta^{15}N_{NH4}$). Assuming that all $\delta^{15}N_{NH4}$ for our samples would have been positive, our assumption of $\delta^{15}N_{NH4}$ values equal to 0 ‰ would tend to underestimate $AF_{15N\text{-}NOxi}$, the initial (in situ) atom fraction ^{15}N of ammonium (Eq. 4), overestimating the actual nitrification rate (see Eq. 3). Examples of high $\delta^{15}N_{NH4}$ enrichment (sometimes greater than 30 ‰) have been reported from hydrodynamically simple estuaries with large point sources of ammonium (Mariotti et al. 1984; Cifuentes et al. 1989; Velinsky et al. 1989; Middelburg and Nieuwenhuize 2001; Sebilo et al. 2006). However, preliminary data from San Francisco Bay indicate a surface water $\delta^{15}N_{NH4}$ range of 6.8 to 17.8 ‰ between stations USGS-6 and USGS-657 from April 2011 to October 2014 ($n = 70$; Carol Kendall et al., personal communication). Altering the initial $\delta^{15}N_{NH4}$ value in our nitrification rate calculations from 0 ‰ to the preliminary maximum of 17.8 ‰ only decreased our calculated rates by 0.0004 to 0.0249 nM day^{-1} (average = 0.0038 ± 0.0045 nM day^{-1}). Even assuming an extreme $\delta^{15}N_{NH4}$ value of 50 ‰, calculated rates decreased by only 0.0012 to 0.0698 nM day^{-1}. Therefore, while our assumption of $\delta^{15}N_{NH4}$ equal to 0 ‰ slightly overestimated our nitrification rate calculations, this bias is not large enough to significantly affect our results.

Ammonia-Oxidizing Microorganisms in Estuary Water Columns Remain Understudied

Relatively few studies have documented the abundance or diversity of ammonia-oxidizing microbes in estuary waters: ammonia-oxidizing populations of the ocean, soils, and estuary sediments have been relatively well characterized (Francis et al. 2005; Nicol et al. 2011), but only a handful of studies have documented these communities in estuary waters, particularly since the discovery of AOA (Bouskill et al. 2012; Hollibaugh et al. 2014; Zhang et al. 2014). Previous work has documented abundant and diverse populations of both AOA and AOB in San Francisco Bay sediments (Francis et al. 2005; Mosier and Francis 2008; Damashek et al. 2015), but nothing is known about the abundance, diversity, or activity of nitrifying microbes in its waters. The wide range of nitrification rates reported in this study reinforces the need to examine ammonia and nitrite oxidizers in estuary waters and to compare their population structure with biogeochemical rates. This lack of knowledge is a clear gap in our understanding of nitrification both in San Francisco Bay and in estuaries worldwide.

Conclusions

This study highlights the significance of pelagic nitrification in estuary waters and its contribution to nitrogen cycling at the land-sea interface. The range of nitrification rates in San Francisco Bay spanned two orders of magnitude, and many samples had rates significantly higher than those typical of seawater. Overall, ammonium, SPM, and temperature were positively correlated with nitrification rates, with a particularly strong relationship between nitrification and SPM, suggesting that turbid estuary waters may be particularly important sites for N cycling. Comparison with data from other estuaries also highlights the importance of SPM and ammonium in driving nitrification rates in many ecosystems, though a diverse array of other factors can have effects on estuarine biogeochemistry, as well. Nitrification in San Francisco Bay, while higher than typical marine rates, appears comparable or lower than rates from other estuarine and coastal ecosystems. This work definitively highlights pelagic nitrification as an important part of the N cycle throughout San Francisco Bay.

Acknowledgments We are grateful to the crews of the R/V *Polaris* and the R/V *Questuary*, as well as Jim Cloern, Tara Schraga, and the rest of the USGS Water Quality of San Francisco Bay group for enabling our participation in cruises and assisting with sample collection. Jason Smith

assisted in cruise planning and sample collection onboard the *Questuary* and, along with Matt Forbes, Carly Buchwald, and Brian Peters, gave valuable help with isotopic measurements. Jim Cloern also provided useful advice in modeling SPM concentrations for *Questuary* sites. Carol Kendall and her group at USGS, particularly Sara Peek, kindly provided preliminary ammonium isotope data prior to publication. Thoughtful comments from two anonymous reviewers, as well as discussions with Alex Parker and Bradley Tolar, greatly improved this manuscript. This work was funded by National Science Foundation Biological Oceanography grant OCE-0847266 (to Chris Francis), and additional salary support came from the 2014–2015 Stanford-USGS Fellowship (to Julian Damashek).

References

Abril, G., S.A. Riou, H. Etcheber, M. Frankignoulle, R. de Wit, and J.J. Middelburg. 2000. Transient, tidal time-scale, nitrogen transformations in an estuarine turbidity maximum—fluid mud system (the Gironde, south-west France). *Estuarine, Coastal and Shelf Science* 50: 703–715. doi:10.1006/ecss.1999.0598.

Alpine, A.E., and J.E. Cloern. 1988. Phytoplankton growth rates in a light-limited environment, San Francisco Bay. *Marine Ecology Progress Series* 44: 167–173. doi:10.3354/meps044167.

Alpine, A.E., and J.E. Cloern. 1992. Trophic interactions and direct physical effects control phytoplankton biomass and production in an estuary. *Limnology and Oceanography* 37: 946–955. doi:10.4319/lo.1992.37.5.0946.

Andersson, M.G.I., N. Brion, and J.J. Middelburg. 2006. Comparison of nitrifier activity versus growth in the Scheldt estuary—a turbid, tidal estuary in northern Europe. *Aquatic Microbial Ecology* 42: 149–158. doi:10.3354/ame042149.

Baer, S.E., T.L. Connelly, R.E. Sipler, P.L. Yager, and D.A. Bronk. 2014. Effect of temperature on rates of ammonium uptake and nitrification in the western coastal Arctic during winter, spring, and summer. *Global Biogeochemical Cycles* 28: 1455–1466. doi:10.1002/2013GB004765.

Beman, J.M., B.N. Popp, and C.A. Francis. 2008. Molecular and biogeochemical evidence for ammonia oxidation by marine Crenarchaeota in the Gulf of California. *The ISME Journal* 2: 429–441. doi:10.1038/ismej.2007.118.

Benner, R., and S. Opsahl. 2001. Molecular indicators of the sources and transformations of dissolved organic matter in the Mississippi river plume. *Organic Geochemistry* 32: 597–611. doi:10.1016/S0146-6380(00)00197-2.

Berounsky, V.M., and S.W. Nixon. 1985. Eutrophication and the rate of net nitrification in a coastal marine ecosystem. *Estuarine, Coastal and Shelf Science* 20: 773–781. doi:10.1016/0272-7714(85)90032-0.

Berounsky, V.M., and S.W. Nixon. 1990. Temperature and the annual cycle of nitrification in waters of Narragansett Bay. *Limnology and Oceanography* 35: 1610–1617. doi:10.4319/lo.1990.35.7.1610.

Berounsky, V.M., and S.W. Nixon. 1993. Rates of nitrification along an estuarine gradient in Narragansett Bay. *Estuaries* 16: 718–730. doi:10.2307/1352430.

Bianchi, M., P. Bonin, and Feliatra. 1994. Bacterial nitrification and denitrification rates in the Rhône River plume (northwestern Mediterranean Sea). *Marine Ecology Progress Series* 103: 197–202. doi:10.3354/meps103197.

Bianchi, M., Feliatra, and D. Lefevre. 1999. Regulation of nitrification in the land-ocean contact area of the Rhône River plume. *Aquatic Microbial Ecology* 18: 301–312. doi:10.3354/ame018301.

Borcard, D., F. Gillet, and P. Legendre. 2011. *Numerical ecology with R*. New York: Springer.

Bouskill, N.J., D. Eveillard, D. Chien, A. Jayakumar, and B.B. Ward. 2012. Environmental factors determining ammonia-oxidizing organism distribution and diversity in marine environments. *Environmental Microbiology* 14: 714–729. doi:10.1111/j.1462-2920.2011.02623.x.

Bower, C.E., and T. Holm-Hansen. 1980. A salicylate-hypochlorite method for determining ammonia in seawater. *Canadian Journal of Fisheries and Aquatic Sciences* 37: 794–798. doi:10.1139/f80-106.

Brand, A., J.R. Lacy, K. Hsu, D. Hoover, S. Gladding, and M.T. Stacey. 2010. Wind-enhanced resuspension in the shallow waters of South San Francisco Bay: mechanisms and potential implications for cohesive sediment transport. *Journal of Geophysical Research* 115, C11024. doi:10.1029/2010JC006172.

Bricker, S.B., B. Longstaff, W. Dennison, A. Jones, K. Boicourt, C. Wicks, and J. Woerner. 2008. Effects of nutrient enrichment in the nation's estuaries: a decade of change. *Harmful Algae* 8: 21–32. doi:10.1016/j.hal.2008.08.028.

Brion, N., G. Billen, L. Guezennec, and A. Ficht. 2000. Distribution of nitrifying activity in the Seine River (France) from Paris to the estuary. *Estuaries* 23: 669–682. doi:10.2307/1352893.

Brion, N., M.G.I. Andersson, M. Elskens, C. Diaconu, W. Baeyens, F. Dehairs, and J.J. Middelburg. 2008. Nitrogen cycling, retention and export in a eutrophic temperate macrotidal estuary. *Marine Ecology Progress Series* 357: 87–99. doi:10.3354/meps07249.

Bristow, L.A., N. Sarode, J. Cartee, A. Caro-Quintero, B. Thamdrup, and F.J. Stewart. 2015. Biogeochemical and metagenomic analysis of nitrite accumulation in the Gulf of Mexico hypoxic zone. *Limnology and Oceanography* 60: 1733–1750. doi:10.1002/lno.10130.

Bronk, D.A., L. Killberg-Thoreson, R.E. Sipler, M.R. Mulholland, Q.N. Roberts, P.W. Bernhardt, M. Garrett, J.M. O'Neil, and C.A. Heil. 2014. Nitrogen uptake and regeneration (ammonium regeneration, nitrification and photoproduction) in waters of the West Florida Shelf prone to blooms of *Karenia brevis*. *Harmful Algae* 38: 50–62. doi:10.1016/j.hal.2014.04.007.

Caffrey, J.M. 1995. Spatial and seasonal patterns in sediment nitrogen remineralization and ammonium concentrations in San Francisco Bay, California. *Estuaries* 18: 219–233. doi:10.2307/1352632.

Caffrey, J.M., J.E. Cloern, and C. Grenz. 1998. Changes in production and respiration during a spring phytoplankton bloom in San Francisco Bay, California, USA: implications for net ecosystem metabolism. *Marine Ecology Progress Series* 172: 1–12. doi:10.3354/meps172001.

Capone, D.G., S.G. Horrigan, S.E. Dunham, and J. Fowler. 1990. Direct determination of nitrification in marine waters by using the short-lived radioisotope of nitrogen, ^{13}N. *Applied and Environmental Microbiology* 56: 1182–1184.

Carini, S.A., M.J. McCarthy, and W.S. Gardner. 2010. An isotope dilution method to measure nitrification rates in the northern Gulf of Mexico and other eutrophic waters. *Continental Shelf Research* 30: 1795–1801. doi:10.1016/j.csr.2010.08.001.

Cébron, A., T. Berthe, and J. Garnier. 2003. Nitrification and nitrifying bacteria in the lower Seine River and estuary (France). *Applied and Environmental Microbiology* 69: 7091–7100. doi:10.1128/AEM.69.12.7091-7100.2003.

Cheng, R.T., and J.W. Gartner. 1985. Harmonic analysis of tides and tidal currents in south San Francisco Bay, California. *Estuarine, Coastal and Shelf Science* 21: 57–74. doi:10.1016/0272-7714(85)90006-X.

Cifuentes, L.A., M.L. Fogel, J.R. Pennock, and J.H. Sharp. 1989. Biogeochemical factors that influence the stable nitrogen isotope ratio of dissolved ammonium in the Delaware Estuary. *Geochimica et Cosmochimica Acta* 53: 2713–2721. doi:10.1016/0016-7037(89)90142-7.

Cloern, J.E. 1987. Turbidity as a control on phytoplankton biomass and productivity in estuaries. *Continental Shelf Research* 7: 1367–1381. doi:10.1016/0278-4343(87)90042-2.

Cloern, J.E., and A.D. Jassby. 2012. Drivers of change in estuarine-coastal ecosystems: discoveries from four decades of study in San Francisco Bay. *Reviews of Geophysics* 50, RG4001. doi:10.1029/2012RG000397.

Cloern, J.E., K.A. Hieb, T. Jacobson, B. Sansó, E. DiLorenzo, M.T. Stacey, J.L. Largier, et al. 2010. Biological communities in San Francisco Bay track large-scale climate forcing over the North Pacific. *Geophysical Research Letters* 37, L21602. doi:10.1029/2010GL044774.

Cole, B.E., and J.E. Cloern. 1984. Significance of biomass and light availability to phytoplankton productivity in San Francisco Bay. *Marine Ecology Progress Series* 17: 15–24. doi:10.3354/meps017015.

Conomos, T.J., R.E. Smith, and J.W. Gartner. 1985. Environmental setting of San Francisco Bay. *Hydrobiologia* 129: 1–12. doi:10.1007/BF00048684.

Dai, M., L. Wang, X. Guo, W. Zhai, Q. Li, B. He, and S.J. Kao. 2008. Nitrification and inorganic nitrogen distribution in a large perturbed river/estuarine system: the Pearl River Estuary, China. *Biogeosciences* 5: 1227–1244. doi:10.5194/bg-5-1227-2008.

Damashek, J., J.M. Smith, A.C. Mosier, and C.A. Francis. 2015. Benthic ammonia oxidizers differ in community structure and biogeochemical potential across a riverine delta. *Frontiers in Microbiology* 5: 743. doi:10.3389/fmicb.2014.00743.

de Bie, M.J.M., M. Starink, H.T.S. Boschker, J.J. Peene, and H.J. Laanbroek. 2002. Nitrification in the Schelde estuary: methodological aspects and factors influencing its activity. *FEMS Microbiology Ecology* 42: 99–107. doi:10.1111/j.1574-6941.2002.tb00999.x.

de Wilde, H.P.J., and M.J.M. de Bie. 2000. Nitrous oxide in the Schelde estuary: production by nitrification and emission to the atmosphere. *Marine Chemistry* 69: 203–216. doi:10.1016/S0304-4203(99)00106-1.

Devlin, M.J., J. Barry, D.K. Mills, R.J. Gowen, J. Foden, D. Sivyer, N. Greenwood, D. Pearce, and P. Tett. 2009. Estimating the diffuse attenuation coefficient from optically active constituents in UK marine waters. *Estuarine, Coastal and Shelf Science* 82: 73–83. doi:10.1016/j.ecss.2008.12.015.

Dore, J.E., and D.M. Karl. 1996. Nitrification in the euphotic zone as a source for nitrite, nitrate, and nitrous oxide at Station ALOHA. *Limnology and Oceanography* 41: 1619–1628. doi:10.4319/lo.1996.41.8.1619.

Enoksson, V. 1986. Nitrification rates in the Baltic Sea: comparison of three isotope techniques. *Applied and Environmental Microbiology* 51: 244–250.

Feliatra, F., and M. Bianchi. 1993. Rates of nitrification and carbon uptake in the Rhône river plume (northwestern Mediterranean Sea). *Microbial Ecology* 26: 21–28. doi:10.1007/BF00166026.

Fitzsimons, M.F., G.E. Millward, D.M. Revitt, and M.D. Dawit. 2006. Desorption kinetics of ammonium and methylamines from estuarine sediments: consequences for the cycling of nitrogen. *Marine Chemistry* 101: 12–26. doi:10.1016/j.marchem.2005.12.006.

Francis, C.A., K.J. Roberts, J.M. Beman, A.E. Santoro, and B.B. Oakley. 2005. Ubiquity and diversity of ammonia-oxidizing archaea in water columns and sediments of the ocean. *Proceedings of the National Academy of Sciences* 102: 14683–14688. doi:10.1073/pnas.0506625102.

Fulweiler, R.W., H.E. Emery, E.M. Heiss, and V.M. Berounsky. 2011. Assessing the role of pH in determining water column nitrification rates in a coastal system. *Estuaries and Coasts* 34: 1095–1102. doi:10.1007/s12237-011-9432-4.

Füssel, J., P. Lam, G. Lavik, M.M. Jensen, M. Holtappels, M. Günter, and M.M.M. Kuypers. 2012. Nitrite oxidation in the Namibian oxygen minimum zone. *The ISME Journal* 6: 1200–1209. doi:10.1038/ismej.2011.178.

Ganju, N.K., and D.H. Schoellhamer. 2008. Lateral variability of the estuarine turbidity maximum in a tidal strait. In *Sediment and ecohydraulics: INTERCOH 2005*, eds. T. Kusuda, H. Yamanishi, J. Spearman, and J. Z. Gailani, 9:339–355. Elsevier. doi:10.1016/S1568-2692(08)80026-5.

Gazeau, F., J.P. Gattuso, J.J. Middelburg, N. Brion, L.S. Schiettecatie, M. Frankignoulle, and A.V. Borges. 2005. Planktonic and whole system metabolism in a nutrient-rich estuary (the Scheldt estuary). *Estuaries* 28: 868–883. doi:10.1007/BF02696016.

Ginestet, P., J.M. Audic, V. Urbain, and J.C. Block. 1998. Estimation of nitrifying bacterial activities by measuring oxygen uptake in the presence of the metabolic inhibitors allylthiourea and azide. *Applied and Environmental Microbiology* 64: 2266–2268.

Glibert, P.M. 2010. Long-term changes in nutrient loading and stoichiometry and their relationships with changes in the food web and dominant pelagic fish species in the San Francisco estuary, California. *Reviews in Fisheries Science* 18: 211–232. doi:10.1080/10641262.2010.492059.

Goosen, N.K., J. Kromkamp, J. Peene, P. van Rijswijk, and P. van Breugel. 1999. Bacterial and phytoplankton production in the maximum turbidity zone of three European estuaries: the Elbe, Westerschelde and Gironde. *Journal of Marine Systems* 22: 151–171. doi:10.1016/S0924-7963(99)00038-X.

Goring, C.A.I. 1962. Control of nitrification by 2-chloro-6-(trichloromethyl) pyridine. *Soil Science* 93: 211–218. doi:10.1097/00010694-196203000-00010.

Grenz, C., J.E. Cloern, S.W. Hager, and B.E. Cole. 2000. Dynamics of nutrient cycling and related benthic nutrient and oxygen fluxes during a spring phytoplankton bloom in South San Francisco Bay (USA). *Marine Ecology Progress Series* 197: 67–80. doi:10.3354/meps197067.

Grundle, D.S., and S.K. Juniper. 2011. Nitrification from the lower euphotic zone to the sub-oxic waters of a highly productive British Columbia fjord. *Marine Chemistry* 126: 173–181. doi:10.1016/j.marchem.2011.06.001.

Hall, G.H. 1984. Measurement of nitrification rates in lake sediments: comparison of the nitrification inhibitors nitrapyrin and allylthiourea. *Microbial Ecology* 10: 25–36. doi:10.1007/BF02011592.

Hallam, S.J., T.J. Mincer, C. Schleper, C.M. Preston, K. Roberts, P.M. Richardson, and E.F. DeLong. 2006. Pathways of carbon assimilation and ammonia oxidation suggested by environmental genomic analyses of marine *Crenarchaeota*. *PLoS Biology* 4, e95. doi:10.1371/journal.pbio.0040095.st003.

Hammond, D.E., C. Fuller, D. Harmon, B. Hartman, M. Korosec, L.G. Miller, R. Rea, S. Warren, W. Berelson, and S.W. Hager. 1985. Benthic fluxes in San Francisco Bay. *Hydrobiologia* 129: 69–90. doi:10.1007/BF00048688.

Hatzenpichler, R., E.V. Lebedeva, E. Spieck, K. Stoecker, A. Richter, H. Daims, and M. Wagner. 2008. A moderately thermophilic ammonia-oxidizing crenarchaeote from a hot spring. *Proceedings of the National Academy of Sciences* 105: 2134–2139. doi:10.1073/pnas.0708857105.

Helder, W., and R.T.P. De Vries. 1983. Estuarine nitrite maxima and nitrifying bacteria (Ems-Dollard estuary). *Netherlands Journal of Sea Research* 17: 1–18.

Hietanen, S., H. Jäntti, C. Buizert, K. Jürgens, M. Labrenz, M. Voss, and J. Kuparinen. 2012. Hypoxia and nitrogen processing in the Baltic Sea water column. *Limnology and Oceanography* 57: 325–337. doi:10.4319/lo.2012.57.1.0325.

Hollibaugh, J.T., and P.S. Wong. 1999. Microbial processes in the San Francisco Bay estuarine turbidity maximum. *Estuaries* 22: 848–862. doi:10.2307/1353066.

Hollibaugh, J.T., S.M. Gifford, M.A. Moran, M.J. Ross, S. Sharma, and B.B. Tolar. 2014. Seasonal variation in the metratranscriptomes of a Thaumarchaeota population from SE USA coastal waters. *The ISME Journal* 8: 685–698. doi:10.1038/ismej.2013.171.

Horak, R.E.A., W. Qin, A.J. Schauer, E.V. Armbrust, A.E. Ingalls, J.W. Moffett, D.A. Stahl, and A.H. Devol. 2013. Ammonia oxidation kinetics and temperature sensitivity of a natural marine community dominated by Archaea. *The ISME Journal* 7: 2023–2033. doi:10.1038/ismej.2013.75.

Horrigan, S.G., and A.L. Springer. 1990. Oceanic and estuarine ammonium oxidation: effects of light. *Limnology and Oceanography* 35: 479–482. doi:10.4319/lo.1990.35.2.0479.

Horrigan, S.G., J.P. Montoya, J.L. Nevins, J.J. McCarthy, H. Ducklow, R. Goericke, and T. Malone. 1990. Nitrogenous nutrient transformations in the spring and fall in the Chesapeake Bay. *Estuarine, Coastal and Shelf Science* 30: 369–391. doi:10.1016/0272-7714(90)90004-B.

Hsiao, S.S.Y., T.C. Hsu, J.W. Liu, X. Xie, Y. Zhang, J. Lin, H. Wang, et al. 2014. Nitrification and its oxygen consumption along the turbid Chang Jiang River plume. *Biogeosciences* 11: 2083–2098. doi:10.5194/bg-11-2083-2014.

Iriarte, A., I. de Madariaga, F. Diez-Garagarza, M. Revilla, and E. Orive. 1996. Primary plankton production, respiration and nitrification in a shallow temperate estuary during summer. *Journal of Experimental Marine Biology and Ecology* 208: 127–151. doi:10.1016/S0022-0981(96)02672-X.

Iriarte, A., A. de la Sota, and E. Orive. 1998. Seasonal variation of nitrification along a salinity gradient in an urban estuary. *Hydrobiologia* 362: 115–126. doi:10.1023/A:1003130516899.

Jacquot, J.E., R.E.A. Horak, S.A. Amin, A.H. Devol, A.E. Ingalls, E.V. Armbrust, D.A. Stahl, and J.W. Moffett. 2014. Assessment of the potential for copper limitation of ammonia oxidation by Archaea in a dynamic estuary. *Marine Chemistry* 162: 37–49. doi:10.1016/j.marchem.2014.02.002.

Jäntti, H., S. Jokinen, and S. Hietanen. 2013. Effect of nitrification inhibitors on the Baltic Sea ammonia-oxidizing community and precision of the denitrifier method. *Aquatic Microbial Ecology* 70: 181–186. doi:10.3354/ame01653.

Jassby, A. 2008. Phytoplankton in the upper San Francisco Estuary: recent biomass trends, their causes and their trophic significance. *San Francisco Estuary and Watershed Science* 6: Article 2.

Jay, D.A., and J.D. Musiak. 1994. Particle trapping in estuarine tidal flows. *Journal of Geophysical Research* 99: 20445–20461. doi:10.1029/94JC00971.

Jørgensen, B.B., M. Bang, and T.H. Blackburn. 1990. Anaerobic mineralization in marine sediments from the Baltic Sea-North Sea transition. *Marine Ecology Progress Series* 59: 39–54. doi:10.3354/meps059039.

Junk, G., and H.J. Svec. 1958. The absolute abundance of the nitrogen isotopes in the atmosphere and compressed gas from various sources. *Geochimica et Cosmochimica Acta* 14: 234–243. doi:10.1016/0016-7037(58)90082-6.

Kahle, D., and H. Wickham. 2013. ggmap: spatial visualization with ggplot2. *The R Journal* 5: 144–161.

Kimmerer, W. 2004. Open water processes of the San Francisco Estuary: from physical forcing to biological responses. *San Francisco Estuary and Watershed Science* 2: Article 1.

Kitidis, V., B. Laverock, L.C. McNeill, A. Beesley, D. Cummings, K. Tait, M.A. Osborn, and S. Widdicombe. 2011. Impact of ocean acidification on benthic and water column ammonia oxidation. *Geophysical Research Letters* 38, L21603. doi:10.1029/2011GL049095.

Lam, P., G. Lavik, M.M. Jensen, J. van de Vossenberg, M. Schmid, D. Woebken, D. Gutiérrez, R. Amann, M.S.M. Jetten, and M.M.M. Kuypers. 2009. Revising the nitrogen cycle in the Peruvian oxygen minimum zone. *Proceedings of the National Academy of Sciences* 106: 4752–4757. doi:10.1073/pnas.0812444106.

Lee, D.Y., D.P. Keller, B.C. Crump, and R.R. Hood. 2012. Community metabolism and energy transfer in the Chesapeake Bay estuarine turbidity maximum. *Marine Ecology Progress Series* 449: 65–82. doi:10.3354/meps09543.

Lees, H. 1952. The biochemistry of nitrifying organisms 1. The ammonia-oxidizing systems of *Nitrosomonas*. *Biochemical Journal* 52: 134–139.

Legendre, L., and M. Gosselin. 1996. Estimation of N or C uptake rates by phytoplankton using ^{15}N or ^{13}C: revisiting the usual computation formulae. *Journal of Plankton Research* 19: 263–271. doi:10.1093/plankt/19.2.263.

Legendre, P., and L. Legendre. 2012. *Numerical ecology*, 3rd ed. San Francisco: Elsevier.

Lehman, P.W., G. Boyer, C. Hall, S. Waller, and K. Gehrts. 2005. Distribution and toxicity of a new colonial *Microcystis aeruginosa* bloom in the San Francisco Bay Estuary, California. *Hydrobiologia* 541: 87–99. doi:10.1007/s10750-004-4670-0.

Lipschultz, F., S.C. Wofsy, and L.E. Fox. 1986. Nitrogen metabolism of the eutrophic Delaware River ecosystem. *Limnology and Oceanography* 31: 701–716. doi:10.4319/lo.1986.31.4.0701.

Mariotti, A., C. Lancelot, and G. Billen. 1984. Natural isotopic composition of nitrogen as a tracer of origin for suspended organic matter in the Scheldt estuary. *Geochimica et Cosmochimica Acta* 48: 549–555. doi:10.1016/0016-7037(84)90283-7.

McCarthy, J.J., W. Kaplan, and J.L. Nevins. 1984. Chesapeake Bay nutrient and plankton dynamics. 2. Sources and sinks of nitrite. *Limnology and Oceanography* 29: 84–98. doi:10.4319/lo.1984.29.1.0084.

McIlvin, M.R., and K.L. Casciotti. 2011. Technical updates to the bacterial method for nitrate isotopic analyses. *Analytical Chemistry* 83: 1850–1856. doi:10.1021/ac1028984.

McKee, L.J., N.K. Ganju, and D.H. Schoellhamer. 2006. Estimates of suspended sediment entering San Francisco Bay from the Sacramento and San Joaquin Delta, San Francisco Bay, California. *Journal of Hydrology* 323: 335–352. doi:10.1016/j.jhydrol.2005.09.006.

Merbt, S.N., D.A. Stahl, E.O. Casamayor, E. Martí, G.W. Nicol, and J.I. Prosser. 2012. Differential photoinhibition of bacterial and archaeal ammonia oxidation. *FEMS Microbiology Letters* 327: 41–46. doi:10.1111/j.1574-6968.2011.02457.x.

Middelburg, J.J., and J. Nieuwenhuize. 2001. Nitrogen isotope tracing of dissolved inorganic nitrogen behaviour in tidal estuaries. *Estuarine, Coastal and Shelf Science* 53: 385–391. doi:10.1006/ecss.2001.0805.

Miranda, J., K.K. Balachandran, R. Ramesh, and M. Wafar. 2008. Nitrification in Kochi backwaters. *Estuarine, Coastal and Shelf Science* 78: 291–300. doi:10.1016/j.ecss.2007.12.004.

Miyazaki, T., E. Wada, and A. Hattori. 1973. Capacities of shallow waters of Sagami Bay for oxidation and reduction of inorganic nitrogen. *Deep Sea Research* 20: 571–577. doi:10.1016/0011-7471(73)90081-8.

Morin, J., and J.W. Morse. 1999. Ammonium release from resuspended sediments in the Laguna Madre estuary. *Marine Chemistry* 65: 97–110. doi:10.1016/S0304-4203(99)00013-4.

Mosier, A.C., and C.A. Francis. 2008. Relative abundance and diversity of ammonia-oxidizing archaea and bacteria in the San Francisco Bay estuary. *Environmental Microbiology* 10: 3002–3016. doi:10.1111/j.1462-2920.2008.01764.x.

Mosier, A.C., M.B. Lund, and C.A. Francis. 2012. Ecophysiology of an ammonia-oxidizing archaeon adapted to low-salinity habitats. *Microbial Ecology* 64: 955–963. doi:10.1007/s00248-012-0075-1.

Murrell, M.C., J.T. Hollibaugh, M.W. Silver, and P.S. Wong. 1999. Bacterioplankton dynamics in northern San Francisco Bay: role of particle association and seasonal freshwater flow. *Limnology and Oceanography* 44: 295–308. doi:10.4319/lo.1999.44.2.0295.

Najjar, R.G., C.R. Pyke, M.B. Adams, D. Breitburg, C. Hershner, M. Kemp, R. Howarth, et al. 2010. Potential climate-change impacts

on the Chesapeake Bay. *Estuarine, Coastal and Shelf Science* 86: 1–20. doi:10.1016/j.ecss.2009.09.026.

Newell, S.E., A.R. Babbin, A. Jayakumar, and B.B. Ward. 2011. Ammonia oxidation rates and nitrification in the Arabian Sea. *Global Biogeochemical Cycles* 25, GB4016. doi:10.1029/2010GB003940.

Newell, S.E., S.E. Fawcett, and B.B. Ward. 2013. Depth distribution of ammonia oxidation rates and ammonia-oxidizer community composition in the Sargasso Sea. *Limnology and Oceanography* 58: 1491–1500. doi:10.4319/lo.2013.58.4.1491.

Nicol, G.W., S. Leininger, and C. Schleper. 2011. Distribution and activity of ammonia-oxidizing archaea in natural environments. In *Nitrification*, ed. B.B. Ward, D.J. Arp, and M.G. Klotz, 157–178. Washington, D.C.: ASM Press.

Novick, E, G M Berg, A Malkassian, and D B Senn. 2014. *Development Plan for the San Francisco Bay Nutrient Monitoring Program*. Contribution No. 724. Richmond CA: San Francisco Estuary Institute.

Oksanen, J, F G Blanchet, P Legendre, P R Minchin, R B O'Hara, G L Simpson, P Solymos, M H H Stevens, and H Wagner. 2013. vegan: Community Ecology Package. R package version 2.0-10: http://CRAN.R-project.org/package=vegan.

Ouverney, C.C., and J.A. Fuhrman. 2000. Marine planktonic archaea take up amino acids. *Applied and Environmental Microbiology* 66: 4829–4833. doi:10.1128/AEM.66.11.4829-4833.2000.

Owens, N.J.P. 1986. Estuarine nitrification: a naturally occurring fluidized bed reaction? *Estuarine, Coastal and Shelf Science* 22: 31–44. doi:10.1016/0272-7714(86)90022-3.

Paerl, H.W. 2009. Controlling eutrophication along the freshwater–marine continuum: dual nutrient (N and P) reductions are essential. *Estuaries and Coasts* 32: 593–601. doi:10.1007/s12237-009-9158-8.

Pakulski, J.D., R. Benner, R. Amon, B. Eadie, and T. Whitledge. 1995. Community metabolism and nutrient cycling in the Mississippi River: evidence for intense nitrification at intermediate salinities. *Marine Ecology Progress Series* 117: 207–218. doi:10.3354/meps117207.

Pakulski, J.D., R. Benner, T. Whitledge, R. Amon, B. Eadie, L. Cifuentes, J. Ammerman, and D. Stockwell. 2000. Microbial metabolism and nutrient cycling in the Mississippi and Atchafalaya River plumes. *Estuarine, Coastal and Shelf Science* 50: 173–184. doi:10.1006/ecss.1999.0561.

Parker, A.E., R.C. Dugdale, and F.P. Wilkerson. 2012. Elevated ammonium concentrations from wastewater discharge depress primary productivity in the Sacramento River and the Northern San Francisco Estuary. *Marine Pollution Bulletin* 64: 574–586. doi:10.1016/j.marpolbul.2011.12.016.

Percuoco, V.P., L.H. Kalnejais, and L.V. Officer. 2015. Nutrient release from the sediments of the Great Bay Estuary, N.H. USA. *Estuarine. Coastal and Shelf Science* 161: 76–87. doi:10.1016/j.ecss.2015.04.006.

Pitcher, A., C. Wuchter, K. Siedenberg, S. Schouten, and J.S. Sinninghe Damsté. 2011. Crenarchaeol tracks winter blooms of ammonia-oxidizing Thaumarchaeota in the coastal North Sea. *Limnology and Oceanography* 56: 2308–2318. doi:10.4319/lo.2011.56.6.2308.

R Core Team. 2014. R: a language and environment for statistical computing. *R Foundation for Statistical Computing, Vienna, Austria*. R Foundation for Statistical Computing, Vienna, Austria: http://www.r-project.org.

Rabalais, N.N., R.E. Turner, R.J. Díaz, and D. Justic. 2009. Global change and eutrophication of coastal waters. *ICES Journal of Marine Science* 66: 1528–1537. doi:10.1093/icesjms/fsp047.

Rivera-Duarte, I., and A.R. Flegal. 1994. Benthic lead fluxes in San Francisco Bay, California, USA. *Geochimica et Cosmochimica Acta* 58: 3307–3313. doi:10.1016/0016-7037(94)90059-0.

Rockström, J., W. Steffen, K. Noone, A. Persson, F.S. Chapin, E.F. Lambin, T.M. Lenton, et al. 2009. A safe operating space for humanity. *Nature* 461: 472–475. doi:10.1038/461472a.

Ruhl, C.A., and D.H. Schoellhamer. 2004. Spatial and temporal variability of suspended-sediment concentration in a shallow estuarine environment. *San Francisco Estuary and Watershed Science* 2: Article 1.

Ruhl, C.A., D.H. Schoellhamer, R.P. Stumpf, and C.L. Lindsay. 2001. Combined use of remote sensing and continuous monitoring to analyse the variability of suspended-sediment concentrations in San Francisco Bay, California. *Estuarine, Coastal and Shelf Science* 53: 801–812. doi:10.1006/ecss.2000.0730.

Santoro, A.E., and K.L. Casciotti. 2011. Enrichment and characterization of ammonia-oxidizing archaea from the open ocean: phylogeny, physiology and stable isotope fractionation. *The ISME Journal* 5: 1796–1808. doi:10.1038/ismej.2011.58.

Santoro, A.E., K.L. Casciotti, and C.A. Francis. 2010. Activity, abundance and diversity of nitrifying archaea and bacteria in the central California Current. *Environmental Microbiology* 12: 1989–2006. doi:10.1111/j.1462-2920.2010.02205.x.

Santoro, A.E., C.M. Sakamoto, J.M. Smith, J.N. Plant, A.L. Gehman, A.Z. Worden, K.S. Johnson, C.A. Francis, and K.L. Casciotti. 2013. Measurements of nitrite production in and around the primary nitrite maximum in the central California Current. *Biogeosciences* 10: 7395–7410. doi:10.5194/bg-10-7395-2013.

Schoellhamer, D.H. 1996. Factors affecting suspended-solids concentrations in South San Francisco Bay, California. *Journal of Geophysical Research* 101: 12087–12095. doi:10.1029/96JC00747.

Schoellhamer, D.H. 2001. Influence of salinity, bottom topography, and tides on locations of estuarine turbidity maxima in northern San Francisco Bay. In *Coastal and estuarine fine sediment processes*, ed. W.H. McAnally and A.J. Mehta, 343–357. Amsterdam: Elsevier. doi:10.1016/S1568-2692(00)80130-8.

Schubel, J.R., and V.S. Kennedy. 1984. The estuary as a filter: an introduction. In *The estuary as a filter*, ed. V.S. Kennedy, 1–11. Orlando: Academic Press. doi:10.1016/B978-0-12-405070-9.50007-4.

Sebilo, M., G. Billen, B. Mayer, D. Billiou, J.B. Grace, J. Garnier, and A. Mariotti. 2006. Assessing nitrification and denitrification in the Seine River and estuary using chemical and isotopic techniques. *Ecosystems* 9: 564–577. doi:10.1007/s10021-006-0151-9.

Sigman, D.M., K.L. Casciotti, M. Andreani, C. Barford, M. Galanter, and J.K. Böhlke. 2001. A bacterial method for the nitrogen isotopic analysis of nitrate in seawater and freshwater. *Analytical Chemistry* 73: 4145–4153. doi:10.1021/ac010088e.

Simon, N.S. 1989. Nitrogen cycling between sediment and the shallow-water column in the transition zone of the Potomac river and estuary. II. The role of wind-driven resuspension and adsorbed ammonium. *Estuarine, Coastal and Shelf Science* 28: 531–547. doi:10.1016/0272-7714(89)90028-0.

Smith, J.M., F.P. Chavez, and C.A. Francis. 2014a. Ammonium uptake by phytoplankton regulates nitrification in the sunlit ocean. *PLoS ONE* 9, e108173. doi:10.1371/journal.pone.0108173.s003.

Smith, J.M., K.L. Casciotti, F.P. Chavez, and C.A. Francis. 2014b. Differential contributions of archaeal ammonia oxidizer ecotypes to nitrification in coastal surface waters. *The ISME Journal* 8: 1704–1714. doi:10.1038/ismej.2014.11.

Smith, J.M., J. Damashek, F.P. Chavez, and C.A. Francis. 2015. Factors influencing nitrification rates and the abundance and transcriptional activity of ammonia-oxidizing microorganisms in the dark northeast Pacific Ocean. *Limnology and Oceanography*. doi:10.1002/lno.10235.

Soetaert, K., J.J. Middelburg, C. Heip, P. Meire, S. Van Damme, and T. Maris. 2006. Long-term change in dissolved inorganic nutrients in the heterotrophic Scheldt estuary (Belgium, The Netherlands). *Limnology and Oceanography* 51: 409–423. doi:10.4319/lo.2006.51.1_part_2.0409.

Somville, M. 1978. A method for the measurement of nitrification rates in water. *Water Research* 12: 843–848. doi:10.1016/0043-1354(78)90036-2.

Somville, M. 1984. Use of nitrifying activity measurements for describing the effect of salinity on nitrification in the Scheldt estuary. *Applied and Environmental Microbiology* 47: 424–426.

Tolar, B B. 2014. The influence of environmental factors including reactive oxygen species on the spatial and temporal distribution of marine *Thaumarchaeota*. Doctoral Thesis, University of Georgia.

Tourna, M., M. Stieglmeier, A. Spang, M. Könneke, A. Schintlmeister, T. Urich, M. Engel, et al. 2011. *Nitrososphaera viennensis*, an ammonia oxidizing archaeon from soil. *Proceedings of the National Academy of Sciences* 108: 8420–8425. doi:10.1073/pnas.1013488108.

Urakawa, H., W. Martens-Habbena, C. Huguet, J.R. de la Torre, A.E. Ingalls, A.H. Devol, and D.A. Stahl. 2014. Ammonia availability shapes the seasonal distribution and activity of archaeal and bacterial ammonia oxidizers in the Puget Sound Estuary. *Limnology and Oceanography* 59: 1321–1335. doi:10.4319/lo.2014.59.4.1321.

Velinsky, D.J., J.R. Pennock, J.H. Sharp, L.A. Cifuentes, and M.L. Fogel. 1989. Determination of the isotopic composition of ammonium-nitrogen at the natural abundance level from estuarine waters. *Marine Chemistry* 26: 351–361. doi:10.1016/0304-4203(89)90040-6.

Veuger, B., A. Pitcher, S. Schouten, J.S. Sinninghe Damsté, and J.J. Middelburg. 2013. Nitrification and growth of autotrophic nitrifying bacteria and Thaumarchaeota in the coastal North Sea. *Biogeosciences* 10: 1775–1785. doi:10.5194/bg-10-1775-2013.

Walters, R.A., R.T. Cheng, and T.J. Conomos. 1985. Time scales of circulation and mixing processes of San Francisco Bay waters. *Hydrobiologia* 129: 13–36. doi:10.1007/BF00048685.

Wankel, S.D., C. Kendall, C.A. Francis, and A. Paytan. 2006. Nitrogen sources and cycling in the San Francisco Bay Estuary: a nitrate dual isotopic composition approach. *Limnology and Oceanography* 51: 1654–1664. doi:10.4319/lo.2006.51.4.1654.

Ward, B.B. 2012. The global nitrogen cycle. In *Fundamentals of geobiology*, eds. A. H. Knoll, D. E. Canfield, and K. O. Konhauser, 36–48. Blackwell Publishing Ltd. doi:10.1002/9781118280874.ch4.

Ward, B.B., and K.A. Kilpatrick. 1990. Relationship between substrate concentration and oxidation of ammonium and methane in a stratified water column. *Continental Shelf Research* 10: 1193–1208. doi:10.1016/0278-4343(90)90016-F.

Ward, B.B., R.J. Olson, and M.J. Perry. 1982. Microbial nitrification rates in the primary nitrite maximum off southern California. *Deep Sea Research* 29: 247–255. doi:10.1016/0198-0149(82)90112-1.

Ward, B.B., K.A. Kilpatrick, E.H. Renger, and R.W. Eppley. 1989. Biological nitrogen cycling in the nitracline. *Limnology and Oceanography* 34: 493–513. doi:10.4319/lo.1989.34.3.0493.

Warner, J.C., D.H. Schoellhamer, C.A. Ruhl, and J.R. Burau. 2004. Floodtide pulses after low tides in shallow subembayments adjacent to deep channels. *Estuarine, Coastal and Shelf Science* 60: 213–228. doi:10.1016/j.ecss.2003.12.011.

Wengrove, M.E., D.L. Foster, L.H. Kalnejais, V. Percuoco, and T.C. Lippmann. 2015. Field and laboratory observations of bed stress and associated nutrient release in a tidal estuary. *Estuarine, Coastal and Shelf Science* 161: 11–24. doi:10.1016/j.ecss.2015.04.005.

Wickham, H. 2009. *ggplot2: elegant graphics for data analysis*. New York: Springer.

Wilkerson, F.P., R.C. Dugdale, V.E. Hogue, and A. Marchi. 2006. Phytoplankton blooms and nitrogen productivity in San Francisco Bay. *Estuaries and Coasts* 29: 401–416. doi:10.1007/BF02784989.

Yigzaw, S K. 2014. Wastewater and water quality changes in lower South San Francisco Bay, 1957-2013. Master's Thesis, San Jose State University.

Zhang, Y., X. Xie, N. Jiao, S.S.Y. Hsiao, and S.J. Kao. 2014. Diversity and distribution of *amoA*-type nitrifying and *nirS*-type denitrifying microbial communities in the Yangtze River estuary. *Biogeosciences* 11: 2131–2145. doi:10.5194/bg-11-2131-2014.

Zuur, A., E.N. Ieno, N. Walker, A.A. Saveliev, and G.M. Smith. 2009. *Mixed effects models and extensions in ecology with R*. New York: Springer.